scientific reports

Check for updates

OPEN

Improved Lyrebird optimization for multi microgrid sectionalizing and cost efficient scheduling of distributed generation

Karthik Nagarajan[1], Arul Rajagopalan[2]✉, Mohit Bajaj[3]✉, Valliappan Raju[4], Vojtech Blazek[5] & Lukas Prokop[5]

The rising energy demand, substantial transmission and distribution losses, and inconsistent power quality in remote regions highlight the urgent need for innovative solutions to ensure a stable electricity supply. Microgrids (MGs), integrated with distributed generation (DG), offer a promising approach to address these challenges by enabling localized power generation, improved grid flexibility, and enhanced reliability. This paper introduces the Improved Lyrebird Optimization Algorithm (ILOA) for optimal sectionalizing and scheduling of multi-microgrid systems, aiming to minimize generation costs and active power losses while ensuring system reliability. To enhance search efficiency, ILOA incorporates the Levy Flight technique for local search, which introduces adaptive step sizes with long-distance jumps, improving the exploration-exploitation balance. Unlike conventional local search strategies that rely on fixed step sizes, Levy Flight prevents premature convergence by allowing the algorithm to escape local optima and explore the solution space more effectively. Additionally, a chaotic sine map is integrated to enhance global search capability, ensuring better diversity and superior optimization performance compared to traditional algorithms. Simulation studies are conducted on a modified 33-bus distribution system segmented into three independent microgrids. The algorithm is evaluated under single-objective scenarios (cost and loss minimization) and a multi-objective optimization framework combining both objectives. In single-objective optimization, ILOA achieves a generation cost of $19,254.64/hr with 0.7118 kW of power loss, demonstrating marginal improvements over the standard Lyrebird Optimization Algorithm and significant gains over Genetic Algorithm (GA) and Jaya Algorithm (JAYA). In multi-objective optimization, ILOA surpasses competing methods by achieving a generation cost of $89,792.18/hr and 10.26 kW of power loss. The optimization results indicate that, for the IEEE-33 bus system without considering EIR, the proposed ILOA algorithm achieves savings of approximately 0.0014%, 0.0041%, and 0.657% in operation costs compared to LOA, JAYA, and GA, respectively, when MG-1, MG-2, and MG-3 are operational. The analysis of real power loss reduction demonstrates that, in the IEEE-33 bus system without considering EIR, the proposed ILOA algorithm effectively minimizes power loss by approximately 0.692%, 1.696%, and 1.962% in comparison to LOA, JAYA, and GA, respectively, under the operational conditions of MG-1, MG-2, and MG-3. Additionally, reliability constraints based on the Energy Index of Reliability (EIR) are effectively incorporated, further validating the robustness of the proposed approach. Considering EIR, the real power loss analysis for the IEEE-33 bus system highlights that the proposed ILOA algorithm achieves a reduction of approximately 1.319%, 2.069%, and 2.134% in comparison to LOA, JAYA, and GA, respectively, under the operational scenario where MG-1, MG-2, and MG-3 are active. The results confirm that ILOA is a highly efficient and reliable solution for distributed generation scheduling and multi-microgrid sectionalizing, showcasing its potential for real-world applications such as dynamic economic dispatch and demand response integration in smart grid systems.

Keywords Lyrebird optimization algorithm, Distributed generators, Multi-microgrids, Optimal scheduling, Generation cost minimization, Active power loss, Multi-objective optimization, Energy index of reliability (EIR)

[1]Department of Electrical and Electronics Engg, Hindustan Institute of Technology and Science, Chennai, Tamil Nadu, India. [2]Centre for Smart Grid Technologies, School of Electrical Engineering, Vellore Institute of Technology,

Chennai, Tamil Nadu 600 127, India. [3]Hourani Center for Applied Scientific Research, Al-Ahliyya Amman University, Amman, Jordan. [4]Director of Research, Perdana University, Kuala Lumpur, Malaysia. [5]ENET Centre, CEET, VSB-Technical University of Ostrava, 708 00 Ostrava, Czech Republic. ✉email: rarul@vit.ac.in; mohitbajaj.ee@geu.ac.in

The contemporary energy scenery is evolving, with a modification towards decentralized energy systems. Microgrids, small-scale power networks encompassing various distributed energy resources, play a pivotal role in this transformation[1,2]. However, managing these interconnected microgrids poses challenges due to their diverse energy sources, demand fluctuations, and the necessity for constant optimization[3,4]. The integration of distributed generation (DG) and microgrids into power systems has garnered significant attention for enhancing grid reliability, reducing emissions, and achieving energy independence. However, the complex interplay of sectionalizing multi-microgrids and optimally scheduling DG units necessitates advanced optimization techniques. Traditional methods often struggle to balance competing objectives such as cost minimization, emission reduction, and reliability improvement. Multi-microgrid systems represent a paradigm shift in the way we conceive, design, and operate power networks[5]. As an evolution of conventional microgrids, which are localized grids capable of operating self-reliantly or in combination with the utility, multi-microgrid systems expand this concept by interconnecting multiple microgrids into a more complex network[6]. Multi-microgrid systems are designed to improve the resilience and flexibility of power distribution[7]. By interconnecting several microgrids, these systems can achieve higher reliability, allowing for more dynamic and robust energy management[8]. Unlike standalone microgrids, multi-microgrid systems emphasize interconnectedness. These systems enable collaboration among individual microgrids, allowing for shared resources, energy trading, and mutual support during contingencies or peak demand periods[9]. Scaling up the concept of microgrids, multi-microgrid systems cater to larger geographical areas, diverse energy sources, and varied load demands[10]. Optimization algorithms play a crucial role in managing multiple objectives such as cost minimization, emission reduction, and system stability across interconnected microgrids[11]. Leveraging renewable energy sources is a cornerstone of multi-microgrid systems. These systems facilitate the incorporation of various non-conventional energy resources, for instance wind, photovoltaic and hydro-electric, across multiple microgrids, enabling a more sustainable and greener energy matrix[12]. Effective communication and control systems are essential for the seamless operation and coordination of multi-microgrid systems[13]. Advanced control strategies, including hierarchical control architectures and decentralized control mechanisms, are implemented for efficient management[14]. Developing sophisticated optimization and scheduling algorithms is critical for achieving the best utilization of resources in multi-microgrid systems. These algorithms consider multiple objectives, uncertainties in renewable energy generation, load variations, and grid stability constraints[15]. Enhancing grid resilience and reliability is a significant challenge. Multi-microgrid systems need to address issues related to grid stability, fault management, and rapid response to disturbances to ensure uninterrupted power supply[16]. Establishment of suitable regulatory frameworks and market structures is necessary to facilitate energy trading, incentivize efficient energy management strategies, and encourage participation from diverse stakeholders in multi-microgrid systems[17]. The integration of optimization techniques within multi-microgrid systems is indispensable, serving as a linchpin for efficient, resilient, and sustainable energy management[18]. These techniques address the complexities inherent in managing multiple interconnected microgrids, ensuring optimal utilization of resources, and meeting various operational objectives. Multi-microgrid systems entail juggling multiple objectives, including cost minimization, emission reduction, reliability enhancement, and grid stability[19]. Optimization techniques provide the framework to balance these conflicting objectives effectively. Optimizing resource allocation, such as distributed generation sources, storage systems, and load management, is essential. These techniques enable the allocation of resources efficiently across interconnected microgrids to meet demand while minimizing costs[20]. The intermittent nature of renewable energy sources adds complexity. Optimization techniques accommodate uncertainties in renewable generation, ensuring optimal scheduling of renewables while maintaining system stability[21]. The long-term multi-objective optimization of renewable distributed generation (DG) power ratings and battery energy storage system (BESS) energy and power ratings in a grid-connected microgrid was carried out using the fuzzified Grey Wolf Optimizer[22]. A comprehensive approach was implemented to optimize the sizing of renewable DGs and BESS in grid-connected microgrids. The optimization framework incorporated multiple objectives, including minimizing total annual costs, emissions, and energy losses, while maximizing annualized benefits by deferring network upgrades. The day-ahead scheduling of microgrids was formulated as a multi-objective optimization problem, considering wind turbines, solar photovoltaics, and energy storage systems (EES)[23]. This was achieved using game theory and a deep learning neural network (DL-NN) forecasting model, which integrated the Wind-Corrected Moving Average (WCMA) technique to predict wind speed, solar radiation, and load demand with improved accuracy.

Recent advancements in microgrid optimization have significantly emphasized cost-efficiency, emission reduction, and system reliability. Paul et al.[24] developed a quantum particle swarm optimization framework for optimizing sustainable energy management in grid-connected microgrids. Their approach simultaneously minimized cost and emissions, integrating renewable sources into a multi-objective optimization setup that addressed environmental and economic performance trade-offs. This study emphasized the role of intelligent algorithms in handling the conflicting objectives of operational cost and carbon footprint in energy systems. Phommixay et al.[25] presented a comprehensive review of cost optimization techniques for microgrids using particle swarm optimization (PSO). They highlighted the evolution of PSO variants and their application in economic dispatch, load scheduling, and system cost reduction. The study underscored the need for more adaptable and hybrid strategies to manage system uncertainties, particularly in renewable-integrated microgrids. Singh et al.[26] introduced a greedy rat swarm optimization algorithm coupled with price-elastic demand response to enhance economic and environmental efficiency in microgrid operation. Their approach incorporated real-time pricing signals, enabling responsive load management and improved system-level optimization through

behavioral modeling of demand-side participants. Nguyen and Crow[27] proposed a stochastic optimization strategy for microgrids with renewable resources, incorporating battery degradation cost into the scheduling problem. Their model addressed the operational uncertainties of wind and solar power while also accounting for lifecycle cost implications of energy storage systems, providing a more holistic economic framework for microgrid planning. In a related study, Singh et al.[28] developed a hybrid demand-side policy for microgrid scheduling that balanced economic and emission objectives. By integrating demand-side management with generation scheduling, their model achieved enhanced flexibility in dispatch decisions, especially under variable generation and load conditions. Selvaraj et al.[29] applied the crow search algorithm for real-time power scheduling in distribution systems to improve microgrid performance. Their metaheuristic strategy focused on dynamic adaptability and convergence speed, demonstrating promising results for real-time operation under changing demand profiles and resource availability. Garcia-Torres et al.[30] examined stochastic optimization of microgrids incorporating hybrid energy storage systems and energy forecast uncertainties. Their study emphasized the significance of accounting for forecast deviations in both demand and renewable generation, which affect the optimal dispatch of storage units for grid flexibility services. Nadimuthu et al.[31] explored the feasibility of renewable energy-based microgrids with vehicle-to-grid (V2G) technology in smart village applications. Their case study from India highlighted how V2G integration can support energy balancing and storage in isolated and rural microgrid setups, demonstrating social and technical viability. Singh et al.[32] proposed a machine learning-based framework for energy management and forecasting in grid-connected microgrids. By leveraging predictive models, their approach improved the scheduling accuracy of distributed energy sources, enabling proactive optimization under uncertain operating conditions. Ott et al.[33] developed a mixed-integer linear programming (MILP) model for restoration planning in multi-microgrid distribution networks. Their framework supported system reconfiguration and restoration following faults, focusing on operational resilience and supply continuity in complex distributed environments. Karthik et al.[34] introduced a chaotic self-adaptive sine cosine algorithm for solving microgrid optimal scheduling problems. The chaotic adaptation enhanced the algorithm's ability to escape local optima and maintain search diversity, making it suitable for multi-objective scenarios involving generation cost and power quality metrics. Abdalla et al.[35] examined optimized economic operation of microgrids that integrate combined cooling, heating, and power (CCHP) systems along with hybrid energy storage. Their model facilitated comprehensive energy flow management and improved economic efficiency in multiservice microgrid applications. Artis et al.[36] proposed a seismic-resilient planning framework for distribution networks with renewable-based multi-microgrids. Their multi-level strategy incorporated structural and operational planning to enhance grid survivability under seismic disturbances, addressing the critical aspect of infrastructure resilience. Rajagopalan et al.[37] developed a multi-objective energy management model for microgrids integrated with electric vehicles, using an iterative map-based crystal structure optimization algorithm. Their approach addressed the operational complexity introduced by mobile storage and dynamic charging demands, while optimizing for cost, emissions, and load balancing. Arefifar et al.[38] investigated the controllability of voltage and current in multi-microgrid smart distribution systems. Their analysis provided insights into hierarchical control strategies and dynamic coordination among interconnected microgrids, enabling improved system stability and regulation. Malik et al.[39] presented an intelligent multi-stage optimization approach for community-based microgrids under the multi-microgrid paradigm. Their method layered multiple decision levels—generation, storage, and load scheduling—achieving fine-grained control over distributed assets in community-scale applications. He et al.[40] proposed an improved genetic algorithm for economic scheduling in multi-microgrid systems. The enhancements in population diversity and crossover strategy led to better convergence and more robust solutions for cost optimization across interconnected grids.

Table 1 presents a comprehensive review of the literature on Multi-Objective Optimal Scheduling of Multi-Microgrids. The review highlights that real power loss is often overlooked as an objective function, despite its impact on system efficiency. This underscores the need for a more comprehensive optimization framework that integrates real power loss for improved practical applicability. The Improved Lyrebird Optimization Algorithm (ILOA) addresses this gap by analyzing seven case studies, demonstrating its ability to enhance system performance. These findings reinforce the importance of considering real power loss and diverse operational conditions to improve the reliability and efficiency of multi-microgrid systems.

The growing adoption of multi-microgrid systems in modern power grids, driven by the demand for resilience, sustainability, and flexibility, has introduced new challenges in distributed generation (DG) scheduling. Interconnected microgrids must balance conflicting objectives, such as minimizing generation costs, reducing power losses, and maintaining system stability under dynamic load conditions. Traditional optimization methods, including Genetic Algorithm (GA) and Jaya Algorithm (JAYA), often struggle with slow convergence, suboptimal solution quality, and limited scalability in large, complex systems. A major limitation is their tendency for premature convergence, restricting their ability to fully explore the solution space.

Additionally, the increasing integration of renewable energy sources introduces variability and uncertainty, complicating stable and cost-effective energy management. Given these challenges, advanced optimization techniques are essential to effectively balance exploration and exploitation, address renewable energy uncertainties, and optimize multi-objective functions in large-scale interconnected microgrid systems.

To enhance the local search efficiency of the Improved Lyrebird Optimization Algorithm (ILOA), the Levy Flight technique was incorporated due to its ability to balance exploration and exploitation effectively. Conventional local search strategies, such as Gaussian-based random walks, often struggle with premature convergence and getting trapped in local optima, limiting their effectiveness in complex optimization problems. In contrast, Levy Flight introduces adaptive step sizes with occasional long-distance jumps, allowing the algorithm to explore the solution space more efficiently while maintaining precise searches in promising regions. This characteristic helps ILOA navigate multi-modal search spaces, leading to faster convergence, improved solution accuracy, and enhanced robustness. By leveraging Levy Flight, ILOA achieves a well-optimized trade-off

References	Year	Problem	Selected energy sources	Energy storage system	Single/multi-microgrid	Suggested approach	Limitations/challenges
[41]	2022	Multi-objective optimal scheduling	WT, PV, MT, FC	Battery	Single MG	Binary Orientation Search Algorithm (BOSA), PSO	High uncertainty in renewable energy outputs and computational burden from stochastic modeling. Power loss not considered
[42]	2020	Multi-objective optimal scheduling	WT, PV	Battery	Multi MG	Chance-constrained programming	Scenario reduction required for computational feasibility. Power loss not included
[43]	2017	Multi-objective energy management	WT, PV, MT, FC	Battery	Single MG	EDNSGA-II	Reinforcement learning models add computational complexity. Power loss excluded
[44]	2022	Operation control of a multi-microgrid system	WT, PV	Battery	Multi MG	Preference-based multi-objective reinforcement learning (PMORL)	Limited generalizability as the proposed MORL method is tested only in specific scenarios. Power loss not addressed
[45]	2018	Multi-objective energy management	WT, PV, FC	Battery	Single MG	MOPSO	Optimization of AC/DC microgrid power management, but cost and power loss not considered
[46]	2024	Optimal dispatch of microgrids under uncertainties	WT, PV	-	Single MG	Triplet-Critics Comprehensive Experience Replay Soft Actor-Critic (TCSAC)	Challenges in handling uncertainties in renewable generation, multi-objective optimization, and reinforcement learning-based dispatch
[47]	2022	Optimal scheduling	WT, PV, MT	Battery	Single MG	Automated Reinforcement Learning-based Multi-period Forecasting	Excludes real power loss consideration in uncertainty modeling for load forecasting and energy generation
[48]	2020	Multi-objective optimal scheduling	WT,PV	Battery	Single MG	Goal Programming	Neglects operating costs and power loss, impacting real-world feasibility
[49]	2016	Optimal Scheduling	WT, PV	Battery	Single MG	Not Specified	Strategic load and generation management focus but lacks cost and power loss analysis
[50]	2021	Optimal scheduling	WT, PV, MT, FC	Battery	Multi MG	Hybrid lexicography-compromise programming	Fair cost allocation mechanisms need improvement despite achieving cost reduction. Power loss not considered
[51]	2023	Optimal scheduling	WT, PV, MT, FC	Battery	Single MG	Slime Mould Algorithm (SMA)	Scalability concerns as the method is tested on a single microgrid setup with limited DG configurations
[52]	2021	Optimal operational energy management and planning	WT, PV, MT, FC	Battery	Single MG	Improved Multi-Objective Differential Evolutionary (IMODE) Optimization Algorithm	Assumes a power factor of one, neglecting reactive power and potential real-world impact. Power loss excluded
[53]	2022	Energy management	WT, PV	Battery	Multi MG	GAMS and CPLEX Solver	Accuracy concerns due to unaccounted power losses; lacks cost-sharing strategies for multi-microgrid operation
[54]	2024	Multi-objective optimal scheduling	WT, PV, Gas Turbine, Diesel Generator	Battery	Single MG	Improved PSO	Geographical and network limitations restrict scalability; substantial grid support required. Power loss not included
[55]	2024	Optimization of multi-energy cloud energy storage	PV,WT, EC,	Hydrogen energy	Multi MG	Multi-agent dual-layer optimization model	Short-term energy storage focus, with minimal exploration of long-term storage solutions. Power loss not addressed
[56]	2023	Day-ahead scheduling	WT, PV, CHP and GB	Hydrogen and Battery	Multi MG	MILP and ε-constraint approach	Uncertainty modeling challenges persist despite stochastic approaches. Power loss not an objective
[57]	2024	Operation optimization and cost allocation for microgrid	WT and PV	Shared hybrid energy storage system (SHESS)	Multi MG	Multi-objective optimization model using Confidence Gap Decision Theory (CGDT) and improved Shapley method	High computational complexity from multi-objective optimization and confidence interval-based uncertainty modeling. Power loss excluded
[58]	2024	Optimization scheduling for multi-microgrids	WT, PV, MT, Diesel Generator, FC	Hybrid Energy Storage System	Multi MG	SOCP and MILP	Requires integration of multiple advanced mathematical techniques for optimization
[59]	2024	Optimal scheduling	WT, PV, GT	Electric energy storage (EES) and thermal energy storage (TES)	Multi MG	Direction Multiplier Method (ADMM) and Column & Constraints Generation (C&CG)	Computationally intensive distributed optimization and income allocation method. Power loss not included
[60]	2024	Stochastic multi-objective sizing optimization	WT, PV	Battery	Single MG	Self-Adaptive Multi-Objective Genetic Algorithm (SAMOGA)	Pareto frontier analysis demands high computational power. Power loss not included

Continued

References	Year	Problem	Selected energy sources	Energy storage system	Single/multi-microgrid	Suggested approach	Limitations/challenges
[61]	2024	Real-time collaborative optimal energy scheduling and dispatching	WT, PV, MT	Battery	Multi MG	Improved cheetah optimizer (ICO) algorithm	Lacks real power loss consideration despite optimizing energy scheduling
[62]	2024	Economic dispatch	Distributed generators	Not explicitly specified	Multi MG	Two-layer coordinated optimization model using a distributed consensus algorithm	Real-time complexity concerns due to computational overhead. Power loss not addressed
[63]	2024	Optimal scheduling	WT, PV, GT	Electrical and Thermal Energy Storage	Multi MG	Chaotic Gaussian Quantum Crayfish Optimization Algorithm	Requires significant computational resources for CGQCOA implementation and real-time data handling. Power loss not included
[64]	2024	Economic optimization scheduling	WT, PV, Diesel Engine	Battery	Multi MG	Constraint Multi-Objective Evolutionary Algorithm based on Decomposition (CMOEAD), NSGA-II	Economic efficiency-focused optimization. Power loss excluded
[65]	2024	Robust collaborative scheduling	WT, PV	Electrical and Thermal Energy Storage	Multi MG	Column and Constraint Generation (C&CG) method	Effectiveness of the CRRD model in heterogeneous microgrid ownership structures remains unexamined
[66]	2024	Operation scheduling of distribution network	WT, PV	Battery	Multi MG	Improved Beluga Whale Optimization (IBWO)	Scalability concerns as IBWO's computational efficiency remains untested on larger networks
[67]	2024	Optimization of energy management (EM) in a microgrid (MG)	WT, PV, MT, FC	Battery	Single MG	Slime Mould Algorithm (SMA)	Power loss not included in the microgrid optimization model
[68]	2024	Optimization of microgrid scheduling for cost and environmental efficiency	WT, PV, GT, Diesel Engine	Battery	Single MG	Improved Goose Algorithm (IGO) with Latin Hypercube Sampling and K-means clustering	Uncertainty in renewable generation and sustainability concerns. Power loss not considered

Table 1. Literature review on multi-objective optimal scheduling of multi-microgrids.

between global and local search, resulting in higher-quality solutions in both single-objective and multi-objective optimization problems. The effectiveness of this approach is demonstrated through comparative analysis, where ILOA consistently outperforms traditional optimization techniques in multi-microgrid scheduling tasks.

The key contributions of this paper are as follows:

- Integrated Levy Flight into the Lyrebird Optimization Algorithm (LOA), significantly improving local search efficiency and accelerating convergence to optimal solutions in multi-microgrid systems.
- Introduced a chaotic sine map to enhance global exploration, ensuring better diversity in the search space and reducing the likelihood of premature convergence.
- Proposed and applied the Improved Lyrebird Optimization Algorithm (ILOA) to a multi-microgrid test system, addressing both single-objective (generation cost minimization) and multi-objective (generation cost and power loss reduction) optimization problems, with a focus on real-world microgrid applications.
- Conducted a thorough comparison of ILOA with traditional algorithms like LOA, Genetic Algorithm (GA), and Jaya Algorithm (JAYA), demonstrating its superior performance in convergence speed, solution quality, and computational efficiency in large-scale systems.
- Validated the robustness of ILOA through extensive simulations, showing its ability to effectively balance multiple conflicting objectives, handle renewable energy uncertainties, and maintain system stability in dynamic microgrid environments.
- Highlighted ILOA's potential for real-world applications in smart grid systems, particularly in dynamic economic dispatch and demand response integration, positioning the algorithm as a practical solution for future energy management challenges.

The manuscript is organized as follows:"Introduction"section introduces the problem of optimizing distributed generation in multi-microgrid systems, providing the motivation and background for the study."Sectionalization of microgrid distribution system"section presents the sectionalization of microgrid distribution systems, explaining how the system operates under normal and fault conditions, and the process of creating self-sufficient microgrids."Mathematical formulation of multi-objective optimal scheduling of distributed generators"section outlines the mathematical formulation of the multi-objective optimal scheduling problem, presenting the objective functions for cost minimization and power loss reduction, as well as the constraints involved."Improved lyrebird optimization algorithm"section details the proposed Improved Lyrebird Optimization Algorithm (ILOA), explaining its structure, including the integration of Levy Flight for local search enhancement and

chaotic sine map for better global exploration."Simulation results and discussion"section presents the simulation results and discussions, comparing the performance of ILOA with traditional algorithms such as LOA, GA, and JAYA, and highlighting its superior performance in both convergence speed and solution quality."Conclusion and directions for future research" section concludes the paper, summarizing the key findings, and suggestsfuture directions for research and the real-world application of ILOA in smart grid systems.

Sectionalization of microgrid distribution system

The sectionalization process of a multi-microgrid system ensures a continuous power supply under both normal and faulty conditions through a self-healing mechanism that autonomously isolates faults while maintaining stable operation in unaffected areas. The primary goal of this approach is to maximize power delivery to consumers by dynamically reconfiguring the network in response to system conditions. During normal operation, control variables such as micro-source allocations across the distribution network are optimized to achieve specific objectives, including minimization of operating costs, reduction of system losses, and voltage deviation control. These objectives can be addressed individually or in combination to enhance overall system performance. The system maintains a radial topology, ensuring stability and effective protection coordination.

When a fault occurs in any microgrid section, the Microgrid Central Controller (MGCC) detects and isolates the affected region using real-time monitoring data. The faulted section is then disconnected from the rest of the system by opening the tie-line static switches, ensuring that power flow is maintained in the non-affected microgrids. If a fault occurs in a single microgrid (e.g., MG-1), it is isolated from MG-2 and MG-3, allowing the unaffected microgrids to continue operating independently. In the case of a multi-area fault, all impacted areas are disconnected, ensuring that only the healthy microgrids remain operational. Upon sectionalization, each microgrid operates independently in islanded mode, supplying its local loads using available distributed generation (DG) resources. The MGCC plays a crucial role in ensuring that each microgrid maintains self-sufficiency in supply and demand while optimizing energy distribution.

Following sectionalization, the distributed generation units are dynamically rescheduled to optimize power supply within the operational microgrids. The optimization process continues to consider the original objective functions, ensuring reliable and cost-effective energy distribution, efficient power balancing, and system resilience under fault conditions. Once the fault is cleared, the system gradually transitions back to its normal state by reclosing the tie-line switches, with the MGCC ensuring the smooth reintegration of previously disconnected microgrids, preventing power surges or instability. This sectionalization strategy enhances grid resilience by minimizing service disruptions, reducing downtime, and ensuring a reliable power supply to the maximum number of consumers. This approach follows established methodologies from prior studies (such as [Ref.52]) while incorporating modifications tailored to our test system.

Mathematical formulation of multi-objective optimal scheduling of distributed generators

The problem formulation of multi-objective optimal scheduling of Distributed Generators (DGs) in a Distribution System entails a nuanced approach aimed at balancing various competing objectives. At its core, this challenge revolves around achieving efficient energy generation and distribution while minimizing operational costs and real power loss. At its core, this challenge revolves around achieving efficient energy generation and distribution while minimizing operational costs and active power loss[69]. In this complex scenario, the distribution system is divided into multi-microgrids, each representing a distinct section with its own set of DGs and loads. The primary objectives to be optimized are the operational costs associated with running the DGs and the reduction of real power loss within each microgrid. To address these objectives, a multi-objective optimization framework is employed. This involves formulating mathematical models that simultaneously optimize the operation of DGs to minimize costs and mitigate real power losses. The formulation process typically involves defining objective functions that quantify the operational costs and real power loss within each microgrid. Constraints are then imposed to ensure the feasibility of solutions, considering factors such as power balance, voltage limits, and DG capacity constraints.

Mitigation of operation cost

The operation costs objective function aims to minimize the expenses associated with running the DGs within the distribution system. This encompasses various factors for instance generation costs, maintenance costs, and operational overheads incurred in managing the generation units. By optimizing the scheduling of DGs, the research seeks to devise strategies that effectively reduce these operation costs, thereby enhancing the economic efficiency of the system. Here, the generation costs for all units are modelled as second-order quadratic equations, where the cost is a function of the active power generated by each unit. The objective function for minimizing these costs is formulated as the summation of the quadratic cost models for each generating unit, articulated as[41]:

$$F\left(P_g\right) = \sum_{j=1}^{k} \left(x_j + y_j P_{gj} + z_j P_{gj}^2\right) \tag{1}$$

Here x_j, y_j, and z_j represent the operational cost coefficients of the jth generating unit. The variable k denotes the total number of committed online generators.

Mitigation of real power loss

Minimizing real power loss, the energy dissipated during electricity flow, is vital for enhancing system efficiency and reliability. The objective function for real power loss focuses on reducing losses through strategic DG scheduling, voltage profile optimization, and network congestion mitigation[41,70].

$$F(P_{loss}) = \sum_{n=1}^{NL} g_n \left[V_j^2 + V_k^2 - 2V_j V_k \cos\left(\delta_j - \delta_k\right)\right] \tag{2}$$

Here, g_n represents the conductance of the nth transmission line connecting bus j to bus k. Additionally, NL signifies the total number of transmission lines.

Constraints ensuring power balance

Power balance constraints enforce the fundamental principle that total power generation must equal total power consumption within each microgrid. These constraints ensure that the energy produced by DGs matches the energy demand from consumers, maintaining system stability and reliability. Neglecting to meet power balance constraints can result in voltage fluctuations, deviations in frequency, and general instability across the grid. Given that the network operates as a radial system, featuring numerous buses and loads within every feeder, it is essential to account for losses in transmission within the system[41].

$$\sum_{i=1}^{m}\sum_{j=1}^{N_G} P_{Gi,j} = \sum_{i=1}^{m} P_{i,demand} + \sum_{i=1}^{m} P_{i,loss} \tag{3}$$

$$\sum_{i=1}^{m}\sum_{j=1}^{N_G} Q_{Gi,j} = \sum_{i=1}^{m} Q_{i,demand} + \sum_{i=1}^{m} Q_{i,loss} \tag{4}$$

Here $P_{Gi,j}$ and $Q_{Gi,j}$ represent the active and reactive power generated by the jth generating unit at bus i respectively. The variables $P_{i,demand}$ and $Q_{i,demand}$ represent the active and reactive power demands at bus i respectively. Similarly $P_{i,loss}$ and $Q_{i,loss}$ denote the active and reactive power losses in the system at bus i. The term N_G refers to the total number of generating units, while m represents the total number of buses in the system. These equations ensure that the total generated power meets the system's load demand while accounting for power losses.

Constraints on generation capacity

Generation capacity constraints limit the maximum amount of power that each DG unit can produce within a given time period. These constraints are essential for preventing overloading of generation units and ensuring that their operation remains within safe operating limits. By adhering to generation capacity constraints, the optimization algorithm can prevent the generation units from operating beyond their rated capacities, thereby safeguarding equipment integrity and reliability. The constraints to ensure power balance are indeed necessary, as they ensure that the total generation from distributed generation (DG) units and other sources matches the total load demand and losses in the network. This is critical for maintaining stable operation and avoiding issues like overloading, under-voltage, or unbalanced power flows. Without these constraints, the optimization results may be infeasible or lead to unstable network operation.

The active power generation output of every generating unit should be controlled within specified minimum and maximum boundaries[41].

$$P_{gimin} \leq P_{gi} \leq P_{gimax} \tag{5}$$

P_{gi} signifies the active power output of ith generating unit while the maximum and minimum active power output are characterized as P_{gimax}, P_{gimin} for the ith generating unit[71].

$$Q_{gimin} \leq Q_{gi} \leq Q_{gimax} \tag{6}$$

Here P_{gimin} and P_{gimax} represent the minimum and maximum active power operational bounds of unit 'j' within MG 'i', respectively. Similarly Q_{gimin} and Q_{gimax} denote the minimum and maximum reactive power operational bounds of unit 'j' within MG 'i'.

Constraints on bus voltages

Bus voltage constraints dictate the permissible voltage levels at various nodes or buses within the distribution network. Maintaining voltage within acceptable limits is crucial for ensuring the proper functioning of electrical equipment and appliances connected to the grid. Violation of bus voltage constraints can result in equipment damage, inefficient operation, and voltage instability. By enforcing bus voltage constraints, the optimization algorithm ensures that the voltage profile across the distribution system remains within specified limits, thus safeguarding the reliability and quality of power supply to consumers[72].

$$V_{gimin} \leq V_{gi} \leq V_{gimax} \tag{7}$$

The above constraint ensures that the voltage magnitude V_{gi} at the generating unit remains within the specified lower V_{gimin} and upper V_{gimax} limits. This maintains system stability and prevents voltage fluctuations that could impact the reliability and efficiency of power distribution.

Energy index of reliability (EIR)

The Energy Index of Reliability (EIR), represented by (ξ), is used as a constraint to assess the reliability of the power supply, indicating the number of customers impacted by supply disruptions. This index measures the dependability of load power delivery within the system by the collective operation of generators. A higher EIR value implies a lower likelihood of customers experiencing interruptions. The EIR is influenced by the Forced Outage Rate (FOR) of the jth generator (Λ) and its output power (P_j). The Forced Outage Rate reflects the probability of a generator failing to meet the required load demand. The mathematical formulation for calculating EIR is provided in Eq. (3.8) as referenced in[19,73].

$$EIR\,(\xi) = 1 - \left(\frac{\sum_{j=1}^{N_G} \Lambda_j P_j}{\sum_{j=1}^{N_G} P_j)} \right) \tag{8}$$

Here Λ_j and P_j represents the forced outage rate and generated output power of jth generating unit correspondingly.

Formulation of multi-objective optimal scheduling problem

The devising of the multi-objective optimal scheduling problem is presented as follows:

In this context, $F\,(P_g)$ represents the objective function aimed at minimizing generation costs, while $F(P_{loss})$ targets the reduction of active power loss, as described in Eq. (2). Various methods exist for tackling multi-objective optimization problems, including the weighted sum methodology[74], evolutionary algorithms[75], and the ε-constraint method[76]. This paper employs the weighted sum approach to address the multi-objective optimal scheduling problem. In this approach, different weights are assigned to the conflicting objectives to generate multiple sets of Pareto optimal solutions. The optimal compromise solution is then selected from these sets based on the weights. By introducing a price penalty factor through h, the multi-objective problem is transformed into a single-objective optimization problem, as depicted in Eq. (8). The process for calculating the value of h is detailed in[77].

In this methodology, the weighting factor w_1 and w_2 indicates the relative importance of each objective function. When w_1 is set to 1 and w_2 is set to 0, the focus is on minimizing generation costs. When w_1 is set to 0 and w_2 is set to 1 the emphasis shifts to minimizing active power loss. For multi-objective optimal scheduling, w_1 and w_2 are gradually varied from 1 to 0, generating a compromise solution at every step.

The multi-objective function minimization using the weighted sum method is defined as follows[78]:

$$F\,(T) = w_1 * F\,(P_g) + h * w_2 * F\,(P_{loss}) \tag{9}$$

where $w_1 + w_2 = 1$

A value for w_1 and w_2 at 0.5 signifies an equal balance between the generation cost and active power loss functions.

Determination of the optimal compromise solution with fuzzy logic

Prior to making a decision, it is essential to determine the most balanced solution from the set of optimal alternatives. The best compromise solution (BCS) is identified using the fuzzy membership methodology where a decrease in w_1 leads to an increase in generation costs and lessening in active power loss. The fuzzy membership approach is employed to identify this ideal compromise[78]. In the jth fitness function, the value f_j for individual k is represented by a membership function μ_j^k which incorporates the inherent uncertainty in the decision maker's judgment, as detailed below[78]:

$$\mu_j^k = \begin{cases} 1 f_j \le f_j^{min} \\ \frac{f_j^{max} - f_j}{f_j^{max} - f_j^{min}} f_j^{min} < f_j < f_j^{max} \\ 0 f_j \ge f_j^{max} \end{cases} \tag{10}$$

Here, f_j^{max} represents the highest value of the jth fitness function, while f_j^{min} denotes its lowest value among the non-dominated solutions. The standardized membership function μ^k is then computed for every non-dominated solution k as follows[78]:

$$\mu^k = \frac{\sum_{j=1}^{N} \mu_j^k}{\sum_{k=1}^{r} \sum_{j=1}^{N} \mu_j^k} \tag{11}$$

In this context, r symbolizes the overall number of non-dominated solutions. The optimum compromise solution is determined by selecting the one with the maximum value of μ^k.

To determine the best compromise solution (BCS) from the complete set of Pareto optimal solutions, the min–max criterion[79] is applied as follows:

$$\max\left(min_j\left(f_r\right)\right) \tag{12}$$

This implies that the solution with the highest value of $min_j\left(f_r\right)$ is considered the best compromise solution. In this study, for objective functions (1) and (2), the normalized fitness values are represented as follows[80]:

$$P_g = f_1 = \frac{P_g - P_g^{max}}{P_g^{min} - P_g^{max}} \tag{13}$$

$$P_{loss,pu} = f_2 = \frac{P_{loss} - P_{loss}^{max}}{P_{loss}^{min} - P_{loss}^{max}} \tag{14}$$

Improved lyrebird optimization algorithm

The Lyrebird Optimization Algorithm (LOA) is a population-based metaheuristic technique inspired by the adaptive behaviors of lyrebirds in nature[81]. When faced with threats, lyrebirds either flee rapidly or remain motionless in a concealed location, demonstrating an effective exploration–exploitation balance. In LOA, each individual represents a lyrebird, forming a population that iteratively searches for optimal solutions.

To enhance LOA's performance, the Improved Lyrebird Optimization Algorithm (ILOA) integrates Levy Flight and a chaotic sine map. Levy Flight enhances exploitation, enabling a more efficient local search and faster convergence, while the chaotic sine map improves exploration, increasing search diversity and reducing premature convergence. Each lyrebird, acting as an agent, determines decision parameters based on its location in the search space. The population is represented as a matrix, where each vector corresponds to a decision variable, with initial positions set randomly as defined by Eq. (16).

$$X = \begin{bmatrix} X_1 \\ \vdots \\ X_j \\ \vdots \\ X_n \end{bmatrix}_{N\times m} = \begin{bmatrix} x_{1,1} & \cdots & x_{1,j} & \cdots & x_{1,m} \\ \vdots & \ddots & \vdots & \iddots & \vdots \\ x_{i,1} & \cdots & x_{i,j} & \cdots & x_{i,m} \\ \vdots & \iddots & \vdots & \ddots & \vdots \\ x_{N,1} & \cdots & x_{N,j} & \cdots & x_{N,m} \end{bmatrix}_{N\times m} \tag{15}$$

$$x_{i,d} = lb_d + r \cdot (ub_d - lb_d) \tag{16}$$

In this context, X represents the ILOA population matrix, where X_I denotes the ith ILOA member (candidate solution). Each X_I represents the dth dimension of the search space where N is the number of lyrebirds, m is the total number of decision variables, r is a random number within the interval $[0,1]$ and lb_d and ub_d denote the lower and upper bounds of the dth decision parameter correspondingly.

Every ILOA member serves as a candidate solution to the problem, and for every member, the objective function of the problem can be computed. Consequently, for every population member, a corresponding value for the objective function is obtained. These objective function values, equal in number to the size of population, can be organized into a vector representation, as per Eq. (17), indicating the set of evaluated objective function values for the problem[81].

$$F = \begin{bmatrix} F_1 \\ \vdots \\ F_i \\ \vdots \\ F_N \end{bmatrix}_{N\times 1} = \begin{bmatrix} F\left(X_1\right) \\ \vdots \\ F\left(X_i\right) \\ \vdots \\ F\left(X_N\right) \end{bmatrix}_{N\times 1} \tag{17}$$

In this context, F represents the vector of fitness function evaluations, with F_i denoting the evaluation of the objective function using the ith ILOA member. These evaluations serve as a measure of the quality of candidate solutions. The optimal solution corresponds to the best evaluated objective function value (associated with the best ILOA member), while the poorest solution corresponds to the worst evaluated objective function value (linked to the worst ILOA member). Additionally, since the lyrebirds'positions in the problem-solving space is adjusted in each iteration and the finest candidate solution must be revised depending on a comparison of objective function values.

Mathematical modeling approach for ILOA

In the proposed ILOA methodology, the adjustment of population member positions occurs iteratively, guided by the mathematical emulation of lyrebird behavior in response to perceived threats. This modeling incorporates two distinct phases: (i) escape and (ii) concealment, mirroring the decision-making process observed in lyrebirds facing danger.

Within the ILOA framework, the decision-making process of lyrebirds, whether to employ escape or concealment strategies when confronted with danger, is replicated using Eq. (18). Equation (18) in the ILOA framework represents the decision-making mechanism inspired by the behavior of lyrebirds when responding to danger. Specifically:

The decision to either escape or conceal is determined by a randomly generated number r_p within the range [0, 1]. Consequently, the position update of each ILOA member is determined solely by either the escape or

concealment phase. If $r_p \leq 0.5$, the position update is governed by Stage-I, corresponding to the"escape"strategy. Otherwise, the position update follows Stage-II, corresponding to the"concealment"strategy. This mechanism mimics how lyrebirds dynamically choose their response based on situational cues. Within the optimization process, these two stages represent different position update strategies tailored to exploration (escape) and exploitation (concealment), ensuring a balanced search process for optimal solutions.

$$X_i = \begin{cases} Based\,on\,Stage-I, & r_p \leq 0.5 \\ Based\,on\,Stage-II, & else, \end{cases} \tag{18}$$

Exploration stage

During this stage of ILOA, the adjustment of population member positions within the search space is depending on simulating the lyrebird's evasive maneuvers from a perilous location to safer zones. The transition of the lyrebird to these secure regions results in substantial alterations to its position, facilitating the exploration of diverse regions within the problem-solving space. This underscores ILOA's capacity for global exploration.

In the design of ILOA, each member identifies safer areas by considering the loci of other population associates with superior fitness function values. Consequently, Eq. (19) can be utilized to determine the set of safe zones for each ILOA member[81].

$$SA_i = \{X_k : F_k < F_i \text{ and } k \neq i, \text{where } i = \{1, 2, \ldots, N\} \text{ and } k \in \{1, 2, \ldots, N\}\} \tag{19}$$

In this context, SA_i denotes the set of secure zones for the *i*th lyrebird, while X_k represents the kth row of the X matrix, where X has a better fitness function value (i.e., F_k) compared to the ith ILOA associate (i.e., $F_k < F_i$).

Within the ILOA framework, it is presumed that the lyrebird arbitrarily selects one of these safe zones for evasion. Following the modeling of lyrebird transposition in this stage, an updated location is computed for each ILOA member by applying Eq. (20). Subsequently, if this new location leads to an enhancement in the fitness function value, it supplants the earlier location of the equivalent associate as per Eq. (15).

$$x_{i,j}^{P1} = x_{i,j} + r_{i,j}.\left(SSA_{i,j} - I_{i,j}.x_{i,j}\right) \tag{20}$$

$$X_i = \begin{cases} X_i^{P1}, & F_i^{P1} \leq F_i, \\ X_i, & else, \end{cases} \tag{21}$$

In this context, SSA_i represents the chosen secure zone for the ith lyrebird, where SSA_i, denotes its jth dimension. X_i^{P1} represents the newly calculated position for the ith lyrebird depending on the escape strategy of the suggested ILOA, with X_i^{P1} representing its jth dimension. *FiP*1 corresponds to its objective function value and $I_{i,j}$ are randomly selected as either 1 or 2[81].

The indiscriminate number in Eq. (20) can be computed utilizing a sine map, with the preliminary values of C_t and a set to 0.36 and 2.8, respectively[82,83]. The sine map introduces a chaotic behavior in the sequence generation, enhancing the algorithm's exploration capability and preventing premature convergence. By iterating through Eq. (22), the sequence of C_t maintains a non-linear and dynamic progression, improving the diversity of solutions in the optimization process.

$$C_{t+1} = \frac{a}{4}\sin\left(\pi C_t\right), 0 < a < 4 \tag{22}$$

where t is the existing iteration number.

Exploitation stage

In the course of this phase of ILOA, the population member's position within the exploration space is adjusted according to the lyrebird's hiding strategy, aiming to seek refuge in nearby secure areas. This strategy involves meticulously surveying the surrounding environment and taking incremental steps to find an optimal hiding spot, resulting in minor adjustments to the lyrebird's position. This characteristic highlights ILOA's proficiency in local exploitation.

In the design of ILOA, the movement of each member towards a nearby suitable hiding area is modeled, and an updated position is computed for every associate using Eq. (23). If this new position enhances the fitness function value, it swaps the preceding location of the respective associate as per Eq. (26).

In this phase, the Levy flight methodology is used to modify the position of the overall finest component[84,85]. Known for its exploratory capabilities, the Levy flight technique is also connected with restricted search[86,87].

$$x_{i,j}^{P2} = x_{i,j} + (1 - 2 \cdot Levy\,(\lambda)) \cdot \frac{ub_j - lb_j}{t} \tag{23}$$

$$Levy\,(\lambda) = 0.01\frac{r_5\sigma}{|r_6|^{\frac{1}{\beta}}} \tag{24}$$

where σ is determined as:

$$\sigma = \left[\Gamma\left(1+\lambda\right)\sin\left(\pi\frac{\lambda}{2}\right) \Big/ \left(\Gamma\left(\frac{1+\lambda}{2}\right)\lambda\left[2^{\frac{(\lambda-1)}{2}}\right]\right)\right]^{1/\lambda} \tag{25}$$

where $\Gamma(x) = (x-1)!$,, r_5 represents the r_6 random numbers in the range [0,1], and $1 < \beta \leq 2$,. In this research, a persistent value of ($\beta = 1.5$) is applied. $\mathrm{Levy}(\lambda)$ relates to the step length realized by the Levy distribution, which has infinite mean and variance for $1 < \lambda < 3$. λ is the distribution factor, and $\Gamma(.)$ signifies the gamma distribution function.

$$X_i = \begin{cases} X_i^{P2}, & F_i^{P2} \leq F_i, \\ X_i, & else \end{cases} \tag{26}$$

In this context, X_i^{P2} represents the newly calculated position for the ith lyrebird depending on the hiding approach of the suggested ILOA, where X_i^{P2} denotes its jth dimension. F_i^{P2} corresponds to its objective function value. Additionally, t denotes the iteration counter.

Iterative process for implementing the ILOA algorithm

After revising the positions of all lyrebirds, the principal iteration of ILOA concludes. Subsequently, the algorithm progresses to the next iteration, where the ILOA population update process, guided by Eqs. (11)–(19), persists until the final iteration. The finest candidate solution is revised and stored during each iteration. Upon the full execution of ILOA, the finest candidate solution accumulated throughout the algorithm's iterations is outputted as the problem solution.

The procedural workflow for implementing the ILOA algorithm is outlined below:

i. Input problem information: Gather details such as the fitness function, constraints, and decision parameters.
ii. Set population and iteration parameters: Determine the number of population associates (lyrebirds) and the total iterations necessary for solving the problem.
iii. Initial population generation: Randomly generate the initial population of lyrebirds and evaluate each lyrebird using the objective function.
iv. Start iterative process: Begin with the first iteration.
v. Update lyrebird positions: Update the locus of the main lyrebird in the problem-solving space. This update considers two strategies, chosen randomly with equal probability depending on Eq. (4):
vi. If the escape approach is chosen, update the position using Eqs. (5)–(7).
vii. If the hide strategy is chosen, update the position using Eqs. (8) and (9).
viii. Update positions for all lyrebirds: Repeat the position update process for all lyrebirds in the population, similar to the first lyrebird.
ix. Complete iteration: Once all lyrebirds'positions are updated, complete the current iteration. Save the best candidate solution based on the objective function evaluations during this iteration.
x. Proceed to the next iteration: Repeat the lyrebird position update process iteratively until the final iteration is reached.
xi. Finalize algorithm execution: After completing all iterations, identify and output the finest solution attained through the algorithm's execution as the elucidation to the specified problem.

This concludes the implementation of the ILOA algorithm, providing the optimal solution based on the specified problem parameters and constraints.

Figure 1 illustrates a systematic flowchart representing the optimization process for power system operation, focusing on balancing generation costs, minimizing losses, and ensuring voltage stability. It integrates load flow analysis, candidate evaluation, and iterative updates to refine solutions based on fitness metrics. The flowchart effectively visualizes the decision-making process, highlighting convergence checks and scenario-specific objective weighting to achieve an optimal configuration. This structured approach ensures efficient handling of computational tasks and adaptable implementation across various case studies.

Evaluation of the proposed ILOA algorithm

To assess the effectiveness of the proposed ILOA algorithm, it is implemented in MATLAB R2023 A and tested on five standard benchmark functions. Its performance is compared against LOA, SCA, FSAPSO, KH, GA, DE, PSO, CLPSO, ICLPSO, FBCLPSO and FBICLPSO algorithms. The results demonstrate that ILOA outperforms all competing methods in terms of the best solution, mean solution, and standard deviation across all benchmark functions, as presented in Table 2.

Simulation results and discussion

The test system utilized in this research is the standard IEEE 33-bus distribution network, with input data obtained from Ref[41]. It is separated into three independent microgrids, while preserving the radial configuration of the system. During the creation of these microgrids, specific modifications were made to the existing 33-bus system, as detailed below. The allocation of active and reactive power loads for each area is also based on the data from Ref[41].

Altered 33-bus distribution test system and microgrid realization

The 33-bus distribution system is partitioned into three microgrids, designated as MG-1, MG-2, and MG-3[55]. The specifics of line status, including reactance and resistance, are obtained from Ref[41]. for both scenarios: mitigation of generation cost and mitigation of active power loss.

To examine the suggested ILOA algorithm, the subsequent conventions are made:

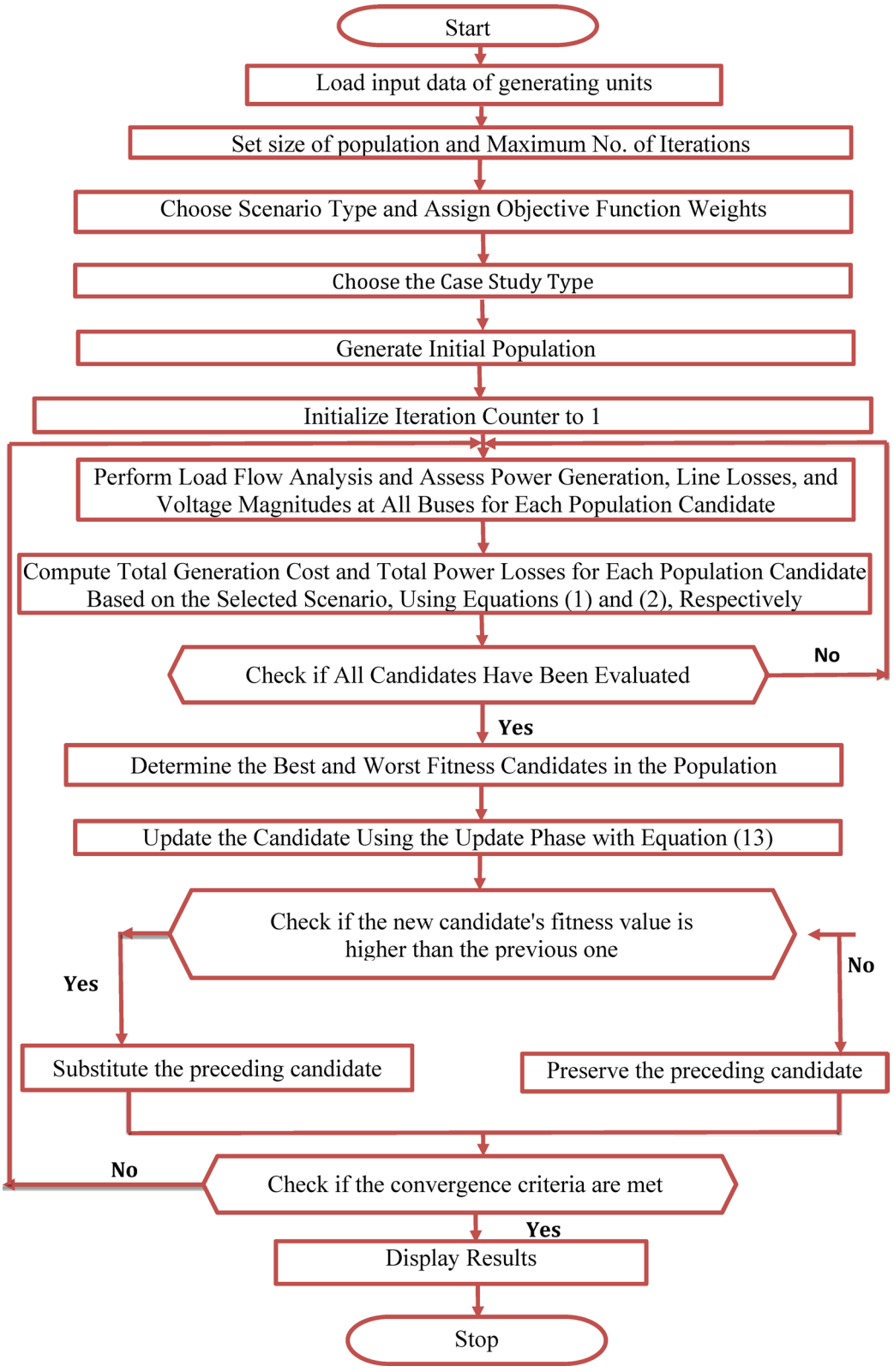

Fig. 1. Flowchart illustrating the optimal scheduling of microgrids using the Improved lyrebird optimization algorithm across diverse scenarios and case studies.

Function	Parameter	Proposed ILOA	LOA	JAYA[41]	SCA [88]	FSAPSO[89]	GA [88]	PSO[88,90]	KH [91]	DE[92]	CLPSO[92]	ICLPSO[92]	FBCLPSO[92]	FBICLPSO[92]	SFLA[90]
Sphere	F_{op}	0.000013	0.000364	NA	NA	2.92E + 01	NA	NA	1.1148E-04	NA	NA	NA	NA	NA	NA
	Mean	0.09875	0.27456	NA	0.3804	4.32E + 01	0.832	0.1045	1.6110E-05	NA	NA	NA	NA	NA	NA
	Std.Dev	0.18547	0.45376	NA	1.0000	1.22E + 01	0.069	0.0541	1.6590E-03	NA	NA	NA	NA	NA	NA
Schwefel 1.2	F_{op}	0.000038	0.000485	NA	NA	NA	NA	NA	NA	0.8889	− 2.0007	1.9851	1.0316	0.7724	NA
	Mean	0.03276	0.38276	NA	0.0000	NA	1.000	0.358	NA	NA	NA	NA	NA	NA	NA
	Std.Dev	0.5847	0.8847	NA	0.7303	NA	0.688	0.879	NA	NA	NA	NA	NA	NA	NA
Rosenbrock	F_{op}	0.000048	0.000534	NA	NA	NA	NA	NA	2.6378E + 01	NA	NA	NA	NA	NA	NA
	Mean	0.06956	0.36478	NA	NA	NA	NA	NA	2.7980E + 01	NA	NA	NA	NA	NA	NA
	Std.Dev	1.0356	2.7454	NA	NA	NA	NA	NA	8.1537E-01	NA	NA	NA	NA	NA	NA
Quartic	F_{op}	0.000061	0.000572	NA	NA	NA	NA	NA	7.0436E + 03	NA	NA	NA	NA	NA	NA
	Mean	0.02674	0.32764	NA	NA	NA	NA	NA	3.2982E + 04	NA	NA	NA	NA	NA	NA
	Std.Dev	1.4837	2.6534	NA	NA	NA	NA	NA	2.7450E + 04	NA	NA	NA	NA	NA	NA
Rastrigin	F_{op}	0.0000132	0.0054373	NA	NA	2.49E + 01	NA	7.1439	7.2421E + 01	2.2200E-11	4.1829E-10	3.8805E-10	3.0409E-10	7.3861E-08	3.5222
	Mean	0.05725	2.04654	NA	0.0005	6.80E + 01	0.667	NA	2.1243E + 01	NA	NA	NA	NA	NA	NA
	Std.Dev	2.01615	4.76353	NA	0.0017	2.07E + 01	0.433	NA	6.7613E + 00	NA	NA	NA	NA	NA	NA

Table 2. Evaluation of the proposed ILOA algorithm on benchmark test functions.

Microgrids	Area wise real power (P) %	Area wise reactive power (Q) %
MG1	12.38	9.57
MG2	37.82	29.57
MG3	49.8	60.87
MG1 & MG2	50.2	39.13
MG2 & MG3	87.62	90.43
MG1 & MG3	62.18	70.43
MG1, MG2 & MG3	100	100

Table 3. Area-wise distribution of real and reactive power load percentages[41].

Active microgrids	Line no	From bus	To bus	R in P.U	X in P.U
MG-1	2	2	3	Line open	Line open
	34	2	23	Line open	Line open
MG-2	2	2	3	Line open	Line open
	22	3	23	Line open	Line open
	25	6	26	Line open	Line open
MG-3	33	25	29	0.001264	0.000644
	22	3	23	Line open	Line open
	25	6	26	Line open	Line open
	34	2	23	Line open	Line open
MG-1 & MG-2	22	3	23	Line open	Line open
	25	6	26	Line open	Line open
	34	2	23	Line open	Line open
MG-2 & MG-3	2	2	3	Line open	Line open
	34	2	23	Line open	Line open
MG-1 & MG-3	33	25	29	0.001264	0.000644
	34	2	23	0.002809	0.00192
	2	2	3	Line open	Line open
	22	3	23	Line open	Line open
	25	6	26	Line open	Line open
MG-1, MG-2 & MG-3	33	25	29	Line open	Line open
	34	2	23	Line open	Line open

Table 4. Line parameters of closed/opened lines for 33-bus system for various cases[41].

- The distributed generators (DGs) used in this study are dispatchable, and their locations remain fixed.
- Isolation and tie-line connections can be established using a static switch.

The population size is fixed as 80, and the maximum no. of iterations is 200. Depending on these optimization attributes, two case studies are implemented to achieve optimal operation of the microgrid, namely cost minimization and real power loss minimization. The subsequent case studies are also examined:

Multiple areas fault:
Case-1: MG-1 is currently operational.
Case-2: MG-2 is currently operational.
Case-3: MG-3 is currently operational.
Single area fault:
Case-4: MG-1 & MG-2 are currently operational.
Case-5: MG-2 & MG-3 are currently operational.
Case-6: MG-1 & MG-3 are currently operational.
Not any fault:
Case-7: MG-1, MG-2 & MG-3 are currently operational.

Table 3 provides the percentage contributions of real power (P) and reactive power (Q) loads from different microgrids (MG1, MG2, MG3) and their combinations. MG1 has the smallest contribution, while MG3 contributes the largest share. The table also shows combined contributions from multiple microgrids, such as MG1 & MG2, MG2 & MG3, and MG1 & MG3. When all three microgrids operate together, they account for 100% of both real and reactive power. This information is essential for understanding how loads are distributed across the system. Table 4 outlines the line parameters (resistance R and reactance X in per-unit) for specific bus connections under various microgrid configurations. It also indicates whether certain lines are opened or closed

S. No	Bus system	Microgrid-1	Microgrid-2	Microgrid-3
1	33- Bus System	1,2,20	3,7,18	23, 26,30

Table 5. Placement of distributed generators (DGs) in a 33-bus system[41].

Bus no	Generator	$x(\$/\mathrm{kW}^2)$	$y(\$/\mathrm{kW})$	$z(\$)$	P_{gmin} (kW)	P_{gmax} (kW)
1	G1	0.0696	26.244	31.67	0	600
2	G2	0.0288	37.697	17.95	0	200
20	G3	0.0468	40.122	22.02	0	100
3	G4	0.0468	40.122	22.02	0	2000
7	G5	0.0268	30.122	22.02	0	800
18	G6	0.0288	37.697	21.95	0	600
23	G7	0.0681	12.441	32.01	0	500
30	G8	0.0288	37.697	21.95	0	5000
26	G9	0.0288	30.697	21.95	0	800

Table 6. Cost coefficients for generators in the 33-bus system[41].

			Line Impedances in p.u		Loads connected to buses					Line impedances in p.u		Loads connected to buses	
Line no	From bus	To bus	$R(\mathrm{p.u})$	$X(\mathrm{p.u})$	$P(\mathrm{kW})$	$Q(\mathrm{kVAR})$	Line no	From bus	To bus	$R(\mathrm{p.u})$	$X(\mathrm{p.u})$	$P(\mathrm{kW})$	$Q(\mathrm{kVAR})$
1	1	2	0.000574	0.000293	100	60	17	17	18	0.004558	0.003574	90	40
2	2	3	0.00307	0.001564	90	40	18	2	19	0.001021	0.000974	90	40
3	3	4	0.002279	0.001161	120	80	19	19	20	0.009366	0.00844	90	40
4	4	5	0.002373	0.001209	60	30	20	20	21	0.00255	0.002979	90	40
5	5	6	0.0051	0.004402	60	20	21	21	22	0.004414	0.005836	90	40
6	6	7	0.001166	0.003853	200	100	22	3	23	0.002809	0.00192	90	50
7	7	8	0.00443	0.001464	200	100	23	23	24	0.005592	0.004415	420	200
8	8	9	0.006413	0.004608	60	20	24	24	25	0.005579	0.004366	420	200
9	9	10	0.006501	0.004608	60	20	25	6	26	0.001264	0.000644	60	25
10	10	11	0.001224	0.000405	45	30	26	26	27	0.00177	0.000901	60	25
11	11	12	0.002331	0.000771	60	35	27	27	28	0.006594	0.005814	60	20
12	12	13	0.009141	0.007192	60	35	28	28	29	0.005007	0.004362	120	70
13	13	14	0.003372	0.004439	120	80	29	29	30	0.00316	0.00161	200	600
14	14	15	0.00368	0.003275	60	10	30	30	31	0.006067	0.005996	150	70
15	15	16	0.004647	0.003394	60	20	31	31	32	0.001933	0.002253	210	100
16	16	17	0.008026	0.010716	60	20	32	32	33	0.002123	0.003301	60	40

Table 7. Data for the 33-bus system[41].

for different scenarios, such as MG1, MG2, MG3, and their combinations. For example, Line 22 (from bus 3 to 23) remains open in many configurations. This data is crucial for analyzing the flexibility and reliability of the system under different microgrid operations. Table 5 presents the placement of distributed generators (DGs) in the 33-bus system for each microgrid. Microgrid-1 has DGs on buses 1, 2, and 20; Microgrid-2 has DGs on buses 3, 7, and 18; and Microgrid-3 has DGs on buses 23, 26, and 30. The strategic placement of DGs ensures optimal power generation and efficient energy distribution across the system. Table 6 provides the cost coefficients and operational constraints for each generator in the system. These coefficients are used to determine the generation costs. Additionally, the table specifies the minimum and maximum generation limits for each generator. The data for the 33-bus distribution system[41] is provided in Table 7. Table 7 provides detailed information on line impedances and connected loads for the 33-bus system. It includes the resistance (R) and reactance (X) of each line in per-unit and the real (P) and reactive (Q) power loads connected to the buses. This data is fundamental for power flow analysis and optimizing system performance.

Single and multi-objective optimization of generation cost and real power loss without EIR

Scenario-I (mitigation of generation cost)

In this scenario, the fitness function was focused exclusively on cost reduction. The operating cost coefficients for each distributed generator (DG) in the 33-bus distribution system were obtained from Ref[41]. For the

Variables	Case_1	Case_2	Case_3	Case_4	Case_5	Case_6	Case_7
P_{G1}	165.2085	–	–	267.3759	–	325.7942	318.9853
P_{G2}	197.5207	–	–	193.0362	–	198.8326	197.7649
P_{G3}	97.9826	–	–	98.87462	–	99.9988	99.1754
P_{G4}	–	274.1286	–	260.5027	339.7109	–	301.8093
P_{G5}	–	660.9784	–	619.5326	747.2081	–	715.0782
P_{G6}	–	479.4947	–	437.4269	539.0284	–	488.5013
P_{G7}	–	–	462.0945	–	437.2187	441.8608	437.8096
P_{G8}	–	–	641.2894	–	543.8913	580.4096	562.3857
P_{G9}	–	–	779.4851	–	702.1872	698.0731	665.7028
P_{Loss}(kW)	0.7118	9.6017	33.0889	11.74892	54.2446	34.9691	72.2125
Q_{Loss}(kVAr)	0.661943	7.682567	26.02592	8.3609	40.9826	25.8093	49.5107
Cost($/hr)	19,254.64	70,900.83	97,915.95	89,443.86	1,68,662.74	1,15,061.66	1,87,645.04

Table 8. optimum values for different case studies in mitigating generation cost for a 33-bus system using the ILOA algorithm.

Optimization approach	Case_1	Case_2	Case_3	Case_4	Case_5	Case_6	Case_7
ILOA	**19,254.64**	**70,900.83**	**97,915.95**	**89,443.86**	**1,68,662.74**	**1,15,061.66**	**1,87,645.04**
LOA	19,255.52	70,901.79	97,917.64	89,445.27	1,68,664.36	1,15,063.75	1,87,647.63
JAYA[41]	19,256.43	70,902.88	97,919.59	89,446.93	1,68,665.57	1,15,067.73	1,87,652.72
GA[41]	19,256.44	70,902.99	97,919.86	89,480.97	1,68,996.73	1, 15,367.94	1,88,885.73

Table 9. Assessment of optimization results for the mitigation of generation cost for various case studies. Bold represent the Significant Value.

minimization of generation cost, when the weighting factor *w* is fixed as 1, the minimum generation cost attained is 19,254.64 $/hr, with a corresponding real power loss of 0.7118 kW for Case-1. Similarly, the optimal generation cost and corresponding real power loss were determined for Case-2 through Case-7. Table 8 displays the optimal power generated by various distributed generators (DGs) for minimizing generation cost using the ILOA. Different generator units are activated based on system requirements, with some cases excluding certain generators to optimize cost and minimize losses. Case_1 has the lowest power losses and the lowest cost, indicating a minimal load scenario. Case_5 experiences the highest losses and the highest operational cost, suggesting a high-demand scenario. Cases with higher power demand (e.g., Case_7) show increased generation costs and losses, requiring multiple generators to meet load demand efficiently. Table 9 reveals that the ILOA algorithm yields better generation cost results, with values of 19,254.64 $/hr, 70,900.83 $/hr, 97,915.95 $/hr, 89,443.86 $/hr, 168,662.74 $/hr, 115,061.66 $/hr and 187,645.94 $/hr for cases 1 through 7, respectively. In comparison, the generation costs obtained using the LOA are 19,255.52 $/hr, 70,901.79 $/hr, 97,917.64 $/hr, 89,445.27 $/hr, 168,664.36 $/hr, 115,063.75 $/hr, and 187,647.63 $/hr for the same cases. In every case study, ILOA achieves the lowest operating cost compared to LOA, JAYA, and GA, making it a cost-effective choice for power system operators, particularly under high-load conditions. The results indicate that ILOA becomes increasingly efficient in reducing operational costs as system size grows. Figure 2 illustrates the convergence behavior of ILOA and LOA for Case-7, showing their progression toward the optimal solution. ILOA converges significantly faster, reaching the optimal value within 26 iterations, whereas LOA requires more iterations and exhibits fluctuations, reflecting instability in its optimization path. These oscillations indicate a less efficient trajectory, making LOA slower and less reliable in achieving convergence. In contrast, ILOA maintains a smooth and consistent search path, demonstrating superior exploration and exploitation capabilities that enable it to locate the global optimum more effectively. Figure 3 further highlights ILOA's advantages, confirming its faster, steadier, and more reliable convergence, making it a more robust optimization approach than standard LOA.

Scenario-II (mitigation of active power loss)

In this state, the objective function considered is solely the mitigation of active power loss. It is presumed that the accessible DGs are dispatchable with stable locations. To minimize active power loss, when the weighting factor *w* is fixed as 0, the lowest active power loss achieved is 0.5846 kW, with a corresponding generation cost of 19,256.84 $/hr for Case-1. Likewise, the optimal real power loss and corresponding generation cost were calculated for Cases 2 through 7. The losses for different case studies, as designated above, are presented in Table 10 for the ILOA algorithm applied to the 33-bus distribution system. Power generation is dynamically adjusted based on system demand, ensuring optimal loss reduction. Case_1 shows the best performance with the lowest active power loss of 0.5846 kW. This suggests that the ILOA algorithm is effective in reducing losses and achieving cost-efficient operations. Case_2 and Case_3 demonstrate higher losses, at 8.5169 kW and 32.6285 kW, respectively, but still outperform the other algorithms in terms of minimizing power loss. Case_4, Case_5,

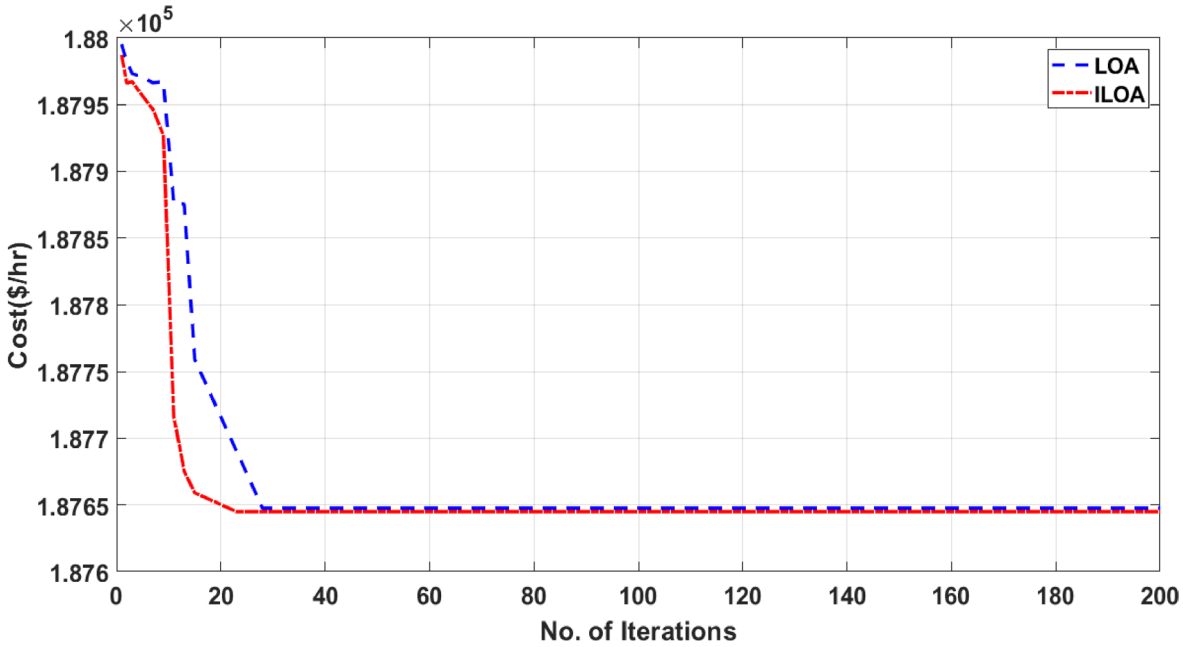

Fig. 2. Convergence characteristics for the mitigation of generation cost for Case_7.

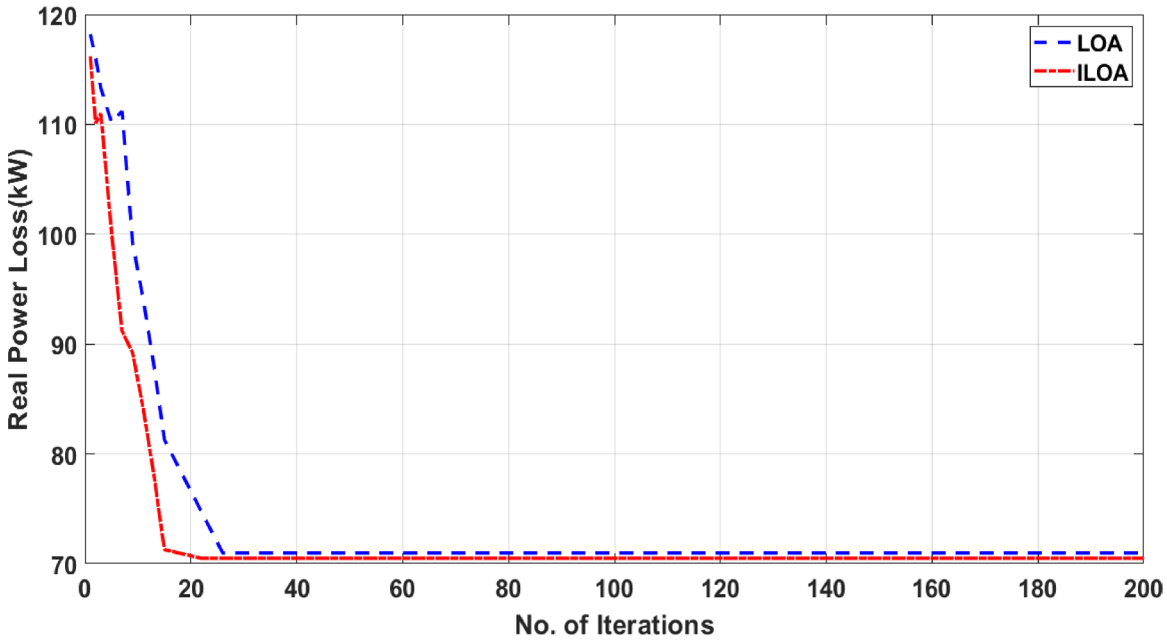

Fig. 3. Convergence characteristics for the mitigation of active power loss for Case_7.

Case_6, and Case_7 all show varying degrees of active power loss with ILOA achieving relatively better results compared to the other methods in most cases.

Table 10 provides the scheduled output power for each distributed generator (DG), along with the system's active and reactive power losses and the overall generation cost. From Table 11, it is observed that the ILOA approach achieves minimum losses of 0.5846 kW, 8.5169 kW, 32.6285 kW, 10.25763 kW, 52.41465 kW, 32.6145 kW, and 70.4914 kW for cases I through VII, respectively. In contrast, the LOA results are 0.6219 kW, 9.0291 kW, 33.1028 kW, 11.3049 kW, 53.0127 kW, 33.1453 kW, and 70.9827 kW for the same cases. The convergence characteristics depicted in Fig. 3 vividly illustrate the superior performance of the Improved Lion Optimization Algorithm (ILOA) in reducing power losses when compared to the conventional Lion Optimization Algorithm (LOA). Moreover Fig. 3 highlights that the ILOA achieves a more significant reduction in active power loss, underscoring its enhanced optimization capabilities. Furthermore, the convergence curve of the proposed

Variables	Case_1	Case_2	Case_3	Case_4	Case_5	Case_6	Case_7
P_{G1}	160.5847	–	–	125.2891	–	337.9032	126.90305
P_{G2}	199.9999	–	–	199.9999	–	175.6285	68.92034
P_{G3}	100	–	–	98.6218	–	99.9999	99.9999
P_{G4}	–	220.3068	–	263.8029	641.30728	–	849.0385
P_{G5}	–	768.0925	–	760.7936	750.18926	–	666.8302
P_{G6}	–	425.1176	–	426.7503	423.90278	–	415.8048
P_{G7}	–	–	500	–	499.5999	499.7999	483.7102
P_{G8}	–	–	582.6285	–	220.30954	797.2546	758.8904
P_{G9}	–	–	800	–	772.10589	433.0284	315.39401
P_{Loss}(kW)	**0.5846**	**8.5169**	**32.6285**	**10.25763**	**52.41465**	**32.6145**	**70.4914**
Q_{Loss}(kVAr)	0.57192	6.40821	26.30278	8.01748	38.8104	24.80247	48.40294
Cost($/hr)	19,256.84	71,408.32	98,124.46	91,346.73	1,77,742.74	1,16,779.38	2,08,978.29

Table 10. Optimum values for different case studies in mitigating active power loss for a 33-bus test system using the ILOA algorithm. Bold represent the Significant Value.

Optimization approach	Case_1	Case_2	Case_3	Case_4	Case_5	Case_6	Case_7
ILOA	**0.5846**	**8.5169**	**32.6285**	**10.25763**	**52.41465**	**32.6145**	**70.4914**
LOA	0.6219	9.0291	33.1028	11.3049	53.0127	33.1453	70.9827
JAYA[41]	0.690474	9.499427	33.673170	12.122236	53.424970	34.635059	71.707680
GA[41]	0.690496	9.520185	33.708979	12.150093	53.469600	34.644690	71.902238

Table 11. Comparison of optimization results for the mitigation of active power loss for various case studies. Bold represent the Significant Value.

Variables	Case_1	Case_2	Case_3	Case_4	Case_5	Case_6	Case_7
P_{G1}	164.50147	–	–	220.48927	–	326.18602	311.20763
P_{G2}	197.26218	–	–	199.90168	–	199.90872	197.30743
P_{G3}	98.89672	–	–	99.98631	–	99.98563	61.28723
P_{G4}	–	275.10182	–	217.27153	414.50982	–	444.29776
P_{G5}	–	688.05947	–	704.28419	696.09275	–	623.10761
P_{G6}	–	451.18401	–	433.33101	453.12971	–	482.19874
P_{G7}	–	–	498.89042	–	499.79081	441.08667	480.29971
P_{G8}	–	–	585.00189	–	543.09156	475.70973	486.46492
P_{G9}	–	–	798.98217	–	701.18758	799.86421	699.90426
P_{Loss}(kW)	**0.66037**	**9.3453**	**32.87448**	**10.26399**	**52.80223**	**32.74098**	**71.07529**
Q_{Loss}(kVAr)	0.653805	7.39104	24.80261	8.93205	37.19802	22.86545	46.02468
Cost($/hr)	**19,254.85**	**70,948.59**	**98,116.47**	**89,792.18**	**1,68,778.26**	**1,15,209.32**	**1,87,892.37**

Table 12. Optimal results for different case studies in reducing generation cost and active power loss for a 33-bus test system using the ILOA algorithm. Bold represent the Significant Value.

ILOA exhibits a smoother and more rapid descent toward the optimal solution in comparison to the LOA. This indicates that the ILOA not only accelerates the convergence process but also ensures greater stability in the optimization trajectory, thereby demonstrating its efficiency and robustness in minimizing active power losses.

Scenario-III (mitigation of generation cost and active power loss)
In this scenario, the optimization of generation cost and reduction of active power loss is considered as a multi-objective problem. Table 12 presents the optimal power generated by various distributed generators (DGs) to mitigate both generation cost and active power loss using the Improved Lyrebird Optimization Algorithm (ILOA) for all the case studies considered. The optimal trade-off between the two objectives was achieved by fine-tuning the weighting factor w from 1 to 0. This table also serves as a foundation for evaluating the finest compromise solution, which aims to balance both minimizing generation costs and active power losses across various operational scenarios.

Table 13 illustrates that the ILOA provides the most favourable compromise solution. This indicates that as the system size grows, the ILOA proves to be more efficient in reducing operational costs.

Optimization approach	ILOA		LOA		JAYA[41]		GA[41]	
Parameters	Generation cost	Active power loss	Generation cost	Active power loss	Generation cost	Active power loss	Generation cost	Active power loss
Case-1	19,254.85	0.66037	19,255.76	0.66507	19,257.51	0.690492	19,257.50	0.690589
Case-2	70,948.59	9.3453	70,952.48	9.4826	70,955.33	9.559371	70,951.86	9.562085
Case-3	98,116.47	32.87448	98,119.26	33.45041	98,120.09	33.679766	98,123.35	33.677627
Case-4	89,792.18	10.26399	89,795.28	11.75026	89,798.02	12.18695	89,991.34	12.301605
Case-5	1,68,778.26	52.80223	1,69,291.27	53.82703	1,69,791.35	54.0869	1,75,424.45	53.4696
Case-6	1,15,209.32	32.74098	1,15,316.28	33.50672	1,15,642.65	34.725637	1,15,623.96	34.744787
Case-7	1,87,892.37	71.07529	1,88,092.15	71.50178	1,89,947.42	72.483248	1,90,814.09	72.076102

Table 13. Assessment of finest compromise solution for the alleviation of generation cost and active power loss for various case studies.

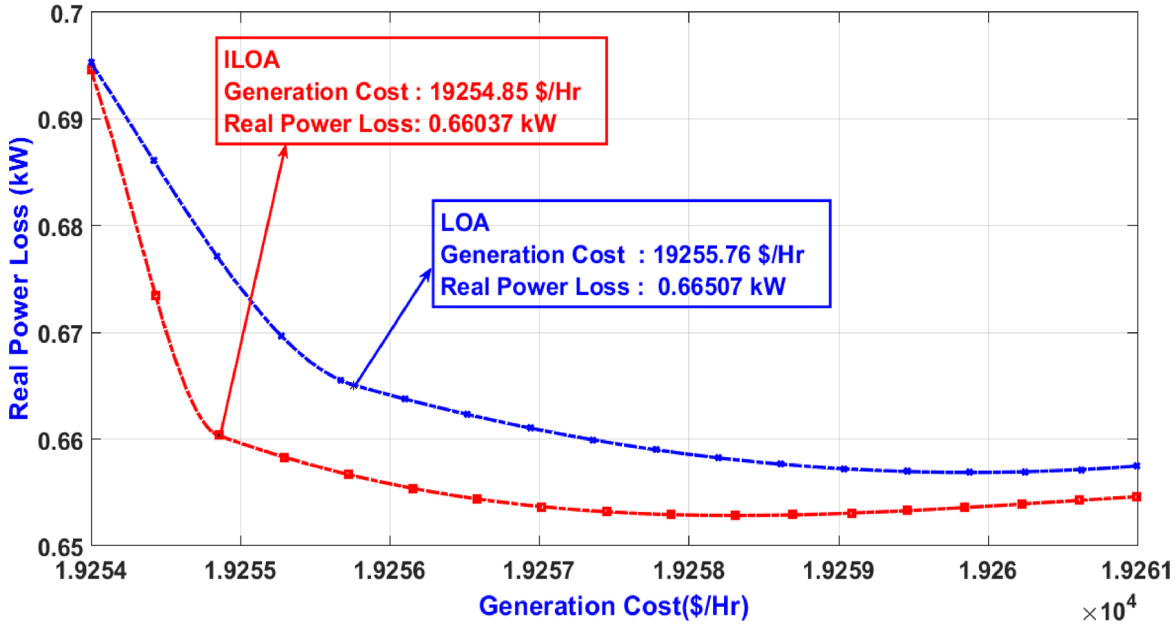

Fig. 4. Pareto front distribution for generation cost and emission mitigation in Case_4.

Figures 4 and 5 provide a comprehensive visual representation of the Pareto fronts obtained for the multi-objective optimization problem, focusing on the simultaneous minimization of generation cost and active power loss reduction. These figures illustrate the comparative performance of both the Improved Lion Optimization Algorithm (ILOA) and the standard Lion Optimization Algorithm (LOA) for Case_4 and Case_7, respectively. A close examination of the Pareto fronts reveals that the ILOA consistently identifies superior trade-off solutions, positioning itself more favourably than the LOA. The optimal points on the Pareto front demonstrate that the ILOA not only surpasses the LOA in achieving lower costs and reduced power losses but also exhibits better solution distribution and diversity. The well-spread, non-dominated solutions offered by the ILOA confirm its robustness and effectiveness in handling the optimization problem. Moreover, these findings underscore the feasibility and reliability of the ILOA in optimizing power distribution within the modified IEEE 33-bus system. By providing a more comprehensive and balanced set of optimal solutions, the ILOA ensures that decision-makers can select the most suitable operational conditions based on system requirements, further validating its superiority over conventional approaches.

Single and multi-objective optimization of generation cost and real power loss with EIR

Table 14 presents the placement and Forced Outage Rate (FOR) of Distributed Generators (DGs) in each microgrid. It outlines the specific buses where DGs are positioned in Microgrid-1 (MG1), Microgrid-2 (MG2), and Microgrid-3 (MG3), along with their associated FOR values. This information is crucial for understanding the reliability and operational constraints of DGs within each microgrid.

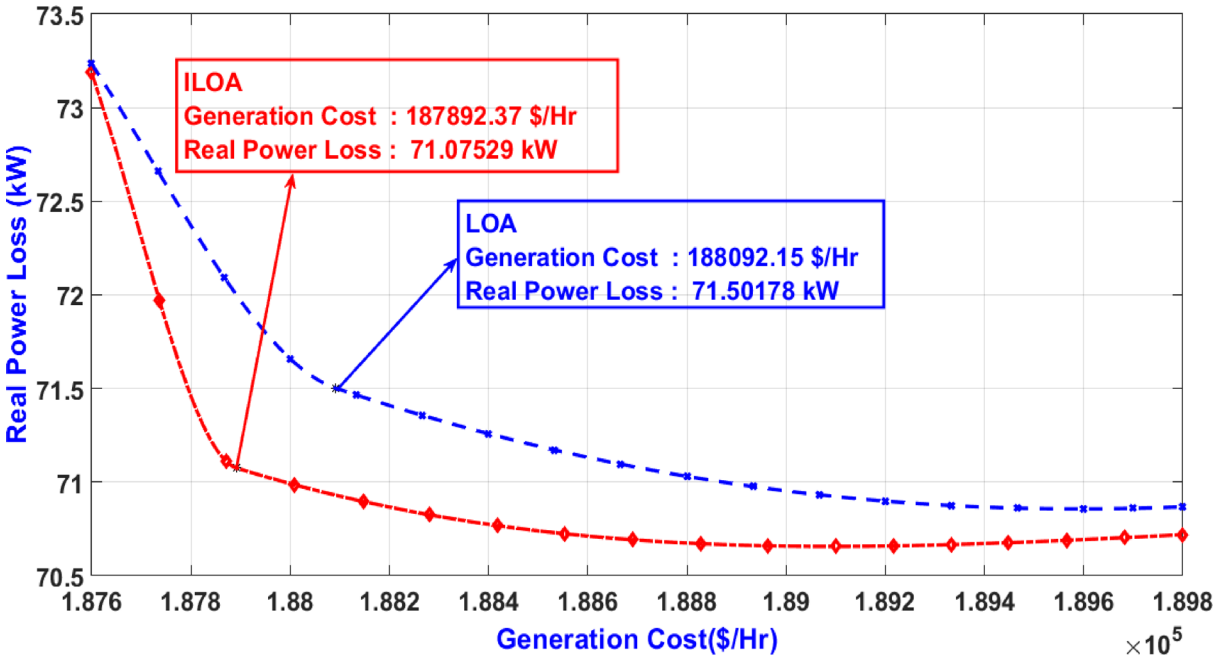

Fig. 5. Pareto front distribution for generation cost and emission mitigation in Case_7.

Microgrid	MG1			MG2			MG3		
DG positioned at bus no	1	2	20	3	7	18	23	30	26
Value of FOR	0.03	0.02	0.05	0.02	0.04	0.05	0.04	0.02	0.05

Table 14. Placement and forced outage rate (FOR) of distributed generators in each microgrid[71].

Variables	Case_1	Case_2	Case_3	Case_4	Case_5	Case_6	Case_7
P_{G1}	163.2135	–	–	159.8243	–	334.7109	352.8911
P_{G2}	198.3098	–	–	199.0002	–	190.0015	198.5023
P_{G3}	99.1254	–	–	57.2097	–	85.5509	45.0027
P_{G4}	–	748.5002	–	788.1023	688.0021	–	663.0001
P_{G5}	–	602.0009	–	568.0017	624.5012	–	584.0023
P_{G6}	–	72.0503	–	110.0007	168.5024	–	178.5011
P_{G7}	–	–	413.5005	–	404.1003	340.0008	384.5006
P_{G8}	–	–	1124.201	–	1180.001	1107.172	1114.207
P_{G9}	–	–	353.5002	–	248.0005	291.0007	279.5008
P_{Loss}(kW)	0.6487	17.5514	41.2018	17.1389	58.1074	38.4371	85.1083
Q_{Loss}(kVAr)	0.6401	13.5008	35.0007	14.2005	45.0004	32.0006	54.0003
Cost($/hr)	**19,255.39**	**87,174.21**	**110,297.19**	**102,014.03**	**196,721.79**	**125,375.57**	**213,370.91**
EIR	0.97	0.97002	0.97002	0.97045	0.97002	0.97087	0.97

Table 15. Scenario-I: operating cost minimization with EIR (Λ) ≥ 0.97. Bold represent the Significant Value.

Scenario-I (mitigation of generation cost)

Table 15 provides a comprehensive analysis of Scenario 1, emphasizing the minimization of operating costs while ensuring an Energy Index of Reliability (EIR) of at least 0.97. It provides variables and their corresponding values across seven case studies, showcasing the results of optimization efforts to minimize operational costs under this scenario. In this context, the fitness function was designed with a primary focus on minimizing operational costs. The operating cost coefficients for each distributed generator (DG) within the 33-bus distribution system were derived from Ref[41]. To reduce generation costs, the weighting factors w_1 and w_2 were assigned values of 1 and 0, respectively. Under this condition, the minimum generation cost achieved was 19,254.64 $/hr, with an associated real power loss of 0.6487 kW for Case_1. Similarly, the optimal generation

Optimization approach	Case_1	Case_2	Case_3	Case_4	Case_5	Case_6	Case_7
ILOA	19,255.39	87,174.21	1,10,297.19	1,02,014.03	1,96,721.79	1,25,375.57	2,13,370.91
LOA	19,256.62	87,175.93	1,10,300.41	1,02,017.62	1,96,724.28	1,25,379.47	2,13,375.18
JAYA[71]	19,256.43	87,175.14	1,10,298.17	1,02,015.60	1,96,723.42	1,25,377.53	2,13,372.95
GA[71]	19,256.44	87,183.16	1,10,310.67	1,06,368.97	1,96,736.99	1,26,040.65	2,28,486.67

Table 16. Assessment of optimization results for the mitigation of generation cost for various case studies.

Variables	Case_1	Case_2	Case_3	Case_4	Case_5	Case_6	Case_7
P_{G1}	162.4273	–	–	166.4283	–	146.5184	133.1347
P_{G2}	199.2165	–	–	199.1372	–	198.1583	197.0927
P_{G3}	99.0321	–	–	58.2891	–	28.0123	99.5017
P_{G4}	–	890.4926	–	823.0278	1193.2715	–	1510.4267
P_{G5}	–	167.2197	–	365.1812	398.3371	–	229.2976
P_{G6}	–	361.1807	–	267.2295	399.4235	–	318.7541
P_{G7}	–	–	499.0784	–	144.4263	170.3321	246.2265
P_{G8}	–	–	1097.2915	–	863.7253	1225.4829	575.5123
P_{G9}	–	–	296.4096	–	310.8512	579.4937	478.8591
P_{Loss}(kW)	**0.6759**	**13.893**	**42.7795**	**14.2931**	**55.0349**	**37.9977**	**73.8054**
Q_{Loss}(kVAr)	0.6554	11.3859	35.4963	11.0792	43.0112	31.5429	52.2238
Cost(\$/hr)	19,256.48	96,126.85	110,927.42	117,977.29	221,844.71	130,615.81	263,906.25
EIR	0.97003	0.97001	0.97003	0.97003	0.97028	0.97016	0.97004

Table 17. Scenario-II: Active power loss minimization with EIR (Λ) ≥ 0.97. Bold represent the Significant Value.

cost and corresponding real power losses were calculated for Cases 2 through 7. Furthermore, Table 15 outlines the optimal power outputs of various DGs aimed at minimizing generation costs using the Improved Lyrebird Optimization Algorithm (ILOA). Additionally, Table 15 demonstrates that the ILOA consistently outperforms in terms of generation cost efficiency. The results obtained using the ILOA for Cases 1 through 7 are 19,255.39 \$/hr, 87,174.21 \$/hr, 110,297.19 \$/hr, 102,014.03 \$/hr, 196,721.79 \$/hr, 125,375.57 \$/hr, and 213,370.91 \$/hr, respectively. In contrast, the generation costs obtained using the standard Lyrebird Optimization Algorithm (LOA) are 19,256.62 \$/hr, 87,175.93 \$/hr, 110,300.41 \$/hr, 102,017.62 \$/hr, 196,724.28 \$/hr, 125,379.4 \$7/hr, and 213,375.18 \$/hr for the same cases. The comparison shows that as system size increases, ILOA significantly outperforms LOA in reducing operational costs. Generation cost minimization was successfully achieved across Cases 1 to 7, while maintaining an Energy Index of Reliability (EIR) of at least 0.97 in every scenario. This demonstrates that ILOA not only lowers costs but also ensures system reliability, guaranteeing stable and secure operation. By keeping EIR at or above 0.97, the optimization strategy effectively balances cost reduction with reliability, ensuring that cost-saving measures do not compromise system stability. As EIR reflects the system's ability to deliver power reliably, maintaining this threshold confirms that economic benefits are achieved without sacrificing performance. Table 16 presents a detailed evaluation of generation cost minimization across different case studies, comparing ILOA with LOA, JAYA, and GA. The results highlight ILOA's superior efficiency, making it a more effective solution for optimizing both economic and operational performance.

Scenario-II (mitigation of active power loss)

Table 17 focuses on Scenario-II, which aims to minimize active power loss with an EIR greater than or equal to 0.97. It lists the variables and their respective values for the seven case studies, demonstrating the optimization results achieved under this scenario. In this scenario, the objective function is exclusively focused on minimizing active power loss. It is assumed that the available distributed generators (DGs) are dispatchable and have fixed locations. The weighting factors w_1 and w_2 were set to 0 and 1, respectively, in order to minimize active power loss. Under these conditions, the minimum active power loss achieved for Case 1 is 0.6759 kW, accompanied by a corresponding generation cost of \$19,256.84 per hour. Similarly, the optimal active power loss and the associated generation costs were determined for Cases 2 through 7. Table 17 presents the active power losses for the various case studies computed using the Improved Lyrebird Optimization Algorithm (ILOA) applied to the 33-bus distribution system. Moreover Table 16 provides detailed information on the scheduled power outputs for each DG, as well as the system's active and reactive power losses and the overall generation costs. The results in Table 17 demonstrate that the ILOA achieves minimal active power losses of 0.6759 kW, 13.893 kW, 42.7795 kW, 14.2931 kW, 55.0349 kW, 37.9977 kW, and 73.8054 kW for Cases 1 through 7, respectively. In comparison, the corresponding results obtained using the Lyrebird Optimization Algorithm (LOA) are 0.6883 kW, 14.591 kW, 43.3917 kW, 14.8704 kW, 55.7019 kW, 38.8627 kW, and 74.7915 kW. Active power loss minimization was successfully achieved across Cases 1 to 7, while maintaining an Energy Index of Reliability (EIR) of at least 0.97.

Optimization approach	Case_1	Case_2	Case_3	Case_4	Case_5	Case_6	Case_7
ILOA	**0.6759**	**13.893**	**42.7795**	**14.2931**	**55.0349**	**37.9977**	**73.8054**
LOA	0.6883	14.591	43.3917	14.8704	55.7019	38.8627	74.7915
JAYA[71]	0.6905	14.6949	43.9116	15.1146	56.5737	41.8670	75.3645
GA[71]	0.6967	14.7158	43.913	15.8492	57.3381	42.4887	75.4144

Table 18. Comparison of optimization results for the mitigation of active power loss for various case studies. Bold represent the Significant Value.

Variables	Case_1	Case_2	Case_3	Case_4	Case_5	Case_6	Case_7
P_{G1}	163.2191	–	–	118.9127	–	325.1905	311.1089
P_{G2}	198.3058	–	–	109.8872	–	199.8926	197.2184
P_{G3}	99.0892	–	–	59.9703	–	99.7518	62.3218
P_{G4}	–	1041.317	–	1160.1892	1005.2901	–	842.2951
P_{G5}	–	107.1183	–	205.0938	295.1185	–	224.1458
P_{G6}	–	270.3028	–	225.1084	255.3091	–	273.0825
P_{G7}	–	–	399.0842	–	149.2891	257.7183	269.2189
P_{G8}	–	–	1164.3372	–	1105.5106	1135.1208	1147.1893
P_{G9}	–	–	327.2107	–	498.2308	330.9716	458.2407
P_{Loss}(kW)	**0.6141**	**13.7381**	**40.6321**	**14.1616**	**53.7482**	**38.6456**	**69.8214**
Q_{Loss}(kVAr)	0.63871	7.36082	24.5083	8.7681	36.4019	22.0472	45.7025
Cost($/hr)	**19,254.78**	**89,388.26**	**110,383.43**	**106,527.38**	**201,843.27**	**127,333.58**	**227,641.59**
EIR	0.97000	0.97277	0.97059	0.97263	0.97048	0.97092	0.97028

Table 19. Scenario 3: Operating cost and active power loss minimization with EIR (Λ) ≥ 0.97. Bold represent the Significant Value.

This ensures that operational efficiency does not compromise system reliability, demonstrating the robustness of the optimization approach. By sustaining an EIR of 0.97 or higher, the system achieves significant power loss reduction while preserving high reliability standards, effectively managing complex power distribution challenges. Table 18 provides a comparative analysis of active power loss minimization results, evaluating the performance of ILOA against LOA, JAYA, and GA. The results highlight ILOA's superior efficiency in reducing power losses, making it a more effective optimization technique compared to conventional methods.

Scenario-III (mitigation of generation cost and active power loss)
Table 19 presents Scenario-III, which addresses the combined objectives of minimizing operating costs and active power losses while ensuring an EIR of 0.97 or higher. It provides detailed results for various variables and their outcomes across seven case studies, highlighting the trade-offs and benefits of addressing both objectives simultaneously. In this scenario, the optimization process is formulated as a multi-objective problem, aiming to minimize both generation cost and active power loss. This approach ensures a balanced trade-off between economic and technical objectives. The optimization is carried out under the condition that the Energy Index of Reliability (EIR) remains greater than 0.97 for all cases, thereby maintaining a high level of reliability in the system. Table 19 provides detailed insights into the optimal power outputs of the distributed generators (DGs) achieved using the Improved Lyrebird Optimization Algorithm (ILOA). The optimal balance between the two objectives was achieved by setting the weighting factors w_1 and w_2 both to 0.5, ensuring the best compromise solution. The Improved Lyrebird Optimization Algorithm (ILOA) produced generation costs of 19,254.78$/hr, 89,388.26 $/hr, 110,383.43 $/hr, 106,527.38 $/hr, 201,843.27 $/hr, 127,333.58 $/hr, and 227,641.59 $/hr, with corresponding real power losses of 0.6141 kW, 13.7381 kW, 40.6321 kW, 14.1616 kW, 53.7482 kW, 38.6456 kW, and 69.8214 kW for Cases 1 through 7, respectively. Table 20 presents the results for all case studies, demonstrating ILOA's effectiveness in reducing both generation costs and active power losses simultaneously. This dual-objective optimization ensures efficient system operation while maintaining reliability constraints, highlighting ILOA's robustness in addressing complex power distribution challenges. The results indicate that ILOA's efficiency improves as system size increases, consistently delivering optimal compromise solutions. Additionally, the Table 20 provides a comparative analysis of ILOA, LOA, and JAYA, showcasing their respective strengths and limitations, with ILOA demonstrating superior optimization performance. ILOA outperforms LOA due to its advanced mechanisms, specifically the chaotic sine map and Levy Flight, which significantly enhance its search capabilities. The chaotic sine map introduces non-linear, dynamic behavior, enabling broader exploration of the solution space while preventing the algorithm from getting trapped in local optima. This controlled randomness improves search diversity, ensuring a more effective and extensive search process. Meanwhile, Levy Flight enhances exploration by allowing larger, adaptive jumps, facilitating the discovery of more optimal solutions. Inspired by natural foraging behavior, this technique enables ILOA to efficiently navigate

Optimization Approach	ILOA		LOA		JAYA[71]	
Parameters	Generation cost	Active power loss	Generation cost	Active power loss	Generation cost	Active power loss
Case_1	19,254.78	0.6141	19,255.83	0.6608	19,256.65	0.69382
Case_2	89,388.26	13.7381	89,400.18	14.8062	89,412.07	15.98204
Case_3	110,383.43	40.6321	110,398.69	42.5196	110,411.04	44.14713
Case_4	106,527.38	14.1616	106,534.27	16.1893	106,546.16	17.79089
Case_5	201,843.27	53.7482	201,861.83	56.5826	201,912.72	58.55761
Case_6	127,333.58	38.6456	127,351.07	40.7025	127,374.03	42.73342
Case_7	227,641.59	69.8214	227,654.46	72.7831	227,690.37	76.27862

Table 20. Assessment of finest compromise solution for the alleviation of generation cost and active power loss for various case studies.

Single objective optimization								
Minimization of operating cost								
			Case_1	Case_2	Case_3	Case_4	Case_5	Case_6	Case_7
Operating Cost ($/hr)	Without EIR	ILOA	**19,254.64**	**70,900.83**	**97,915.95**	**89,443.86**	**168,662.74**	**115,061.66**	**187,645.04**
		LOA	19,255.52	70,901.79	97,917.64	89,445.27	168,664.36	115,063.75	187,647.63
		JAYA[41]	19,256.43	70,902.88	97,919.59	89,446.93	168,665.57	115,067.73	187,652.72
		GA[41]	19,256.44	70,902.99	97,919.86	89,480.97	168,996.73	115,367.94	188,885.73
	With EIR	ILOA	**19,255.39**	**87,174.21**	**110,297.19**	**102,014.03**	**196,721.79**	**125,375.57**	**213,370.91**
		LOA	19,256.62	87,175.93	110,300.41	102,017.62	196,724.28	125,379.47	213,375.18
		JAYA[71]	19,256.43	87,175.14	110,298.17	102,015.60	196,723.42	125,377.53	213,372.95
		GA[71]	19,256.44	87,183.16	110,310.67	106,368.97	196,736.99	126,040.65	228,486.67
Minimization of real power loss								
			Case_1	Case_2	Case_3	Case_4	Case_5	Case_6	Case_7
Real Power Loss (kW)	Without EIR	ILOA	**0.5846**	**8.5169**	**32.6285**	**10.25763**	**52.41465**	**32.6145**	**70.4914**
		LOA	0.6219	9.0291	33.1028	11.3049	53.0127	33.1453	70.9827
		JAYA[41]	0.690474	9.499427	33.673170	12.122236	53.42497	34.635059	71.707680
		GA[41]	0.690496	9.520185	33.708979	12.150093	53.46960	34.644690	71.902238
	With EIR	ILOA	**0.6759**	**13.893**	**42.7795**	**14.2931**	**55.0349**	**37.9977**	**73.8054**
		LOA	0.6883	14.591	43.3917	14.8704	55.7019	38.8627	74.7915
		JAYA[71]	0.6905	14.6949	43.9116	15.1146	56.5737	41.8670	75.3645
		GA[71]	0.6967	14.7158	43.913	15.8492	57.3381	42.4887	75.4144

Table 21. Comparison of EIR values for optimal dg scheduling across different scenarios in the altered 33-bus system with and without the reliability criterion (single-objective optimization). Bold represent the Significant Value.

multi-modal search spaces, improving both solution quality and convergence speed. By integrating these two mechanisms, ILOA achieves a more balanced and robust optimization process, outperforming standard LOA in solving complex, multi-objective problems. These enhancements make ILOA a highly effective approach for optimizing large-scale power distribution systems compared to traditional algorithms.

Analysis of results

A comprehensive analysis of distributed generation (DG) scheduling is presented, utilizing various optimization algorithms within an altered 33-bus electrical distribution system. The study is organized across multiple case studies and divided into two main optimization strategies: single-objective optimization and multi-objective optimization. Table 21 and 22 offer an extensive dataset, examining operating costs and real power losses across different scenarios, both with and without the Enhanced Index of Reliability (EIR) criterion. Table 20 showcases the performance of the proposed Improved Lyrebird Optimization Algorithm (ILOA) alongside the Lyrebird Optimization Algorithm (LOA), JAYA, and Genetic Algorithm (GA) across seven distinct case studies. These results are compared for scenarios with and without the inclusion of EIR as a scheduling criterion. The EIR values for optimal scheduling without considering the EIR criterion have been derived based on the DG power outputs from the test results summarized in Tables 15, 16, 17, 18, 19 and 20. Furthermore, Table 21 highlights that incorporating the EIR criterion into the scheduling process ensures that DGs are optimally scheduled to meet the reliability requirement, in addition to achieving the desired minimization objectives. This approach enhances system performance by simultaneously addressing reliability and operational efficiency.

Multi objective optimization									
Best compromise solution									
			Case_1	Case_2	Case_3	Case_4	Case_5	Case_6	Case_7
Without EIR	ILOA	Cost ($/hr)	19,254.85	70,948.59	98,116.47	89,792.18	1,68,778.26	1,15,209.32	1,87,892.37
		Real Power Loss (kW)	0.66037	9.3453	32.87448	10.26399	52.80223	32.74098	71.07529
	LOA	Cost ($/hr)	19,255.76	70,952.48	98,119.26	89,795.28	1,69,291.27	1,15,316.28	1,88,092.15
		Real Power Loss (kW)	0.66507	9.4826	33.45041	11.75026	53.82703	33.50672	71.50178
	JAYA[41]	Cost ($/hr)	19,257.51	70,955.33	98,120.09	89,798.02	1,69,791.35	1,15,642.65	1,89,947.42
		Real Power Loss (kW)	0.690492	9.559371	33.67977	12.18695	54.0869	34.725637	34.744787
	GA[41]	Cost ($/hr)	19,257.50	70,951.86	98,123.35	89,991.34	1,75,424.45	1,15,623.96	1,90,814.09
		Real Power Loss (kW)	0.690589	9.562085	33.67763	12.30161	53.4696	72.483248	72.076102
With EIR	ILOA	Cost ($/hr)	19,254.8	89,388.3	1,10,383	1,06,527	2,01,843	1,27,334	2,27,642
		Real Power Loss (kW)	0.6141	13.7381	40.6321	14.1616	53.7482	38.6456	69.8214
	LOA	Cost ($/hr)	19,255.8	89,400.2	1,10,399	1,06,534	2,01,862	1,27,351	2,27,654
		Real Power Loss (kW)	0.6608	14.8062	42.5196	16.1893	56.5826	40.7025	72.7831
	JAYA[71]	Cost ($/hr)	19,256.7	89,412.1	1,10,411	1,06,546	2,01,913	1,27,374	2,27,690
		Real Power Loss (kW)	0.69382	15.982	44.1471	17.7909	58.5576	42.7334	76.2786

Table 22. Comparison of EIR values for optimal DG Scheduling across different scenarios in the altered 33-bus system with and without the reliability criterion (multi-objective optimization).

The results are divided into two scenarios: without EIR and with EIR. Across all cases, the inclusion of EIR results in higher operating costs, indicating that reliability considerations introduce additional operational expenses. The operating cost varies significantly across the different cases. Among the algorithms, ILOA consistently yields lower operating costs compared to LOA, JAYA, and GA, making it a potentially more cost-effective choice for DG scheduling. A similar trend is observed for real power loss minimization, where the inclusion of EIR generally leads to higher losses. The real power loss values vary across the cases, with Case_1 showing the lowest losses (around 0.58 kW without EIR and 0.67 kW with EIR), whereas Case_7 has significantly higher losses (70.49 kW without EIR and 73.80 kW with EIR). Among the optimization algorithms, GA and JAYA tend to exhibit slightly higher power losses compared to ILOA and LOA, although the differences are marginal in certain cases.

Table 22 extends the analysis to a multi-objective framework, considering a compromise between operating cost and real power loss. The evaluation follows the same seven-case structure, comparing the four optimization techniques with and without EIR. Without EIR, the operating costs are significantly lower across all cases compared to the EIR-included scenarios. In higher complexity cases like Case_5 and Case_7, the cost increase is more substantial. For example, in Case_7, the cost rises from 1,87,892.37 $/hr (ILOA) without EIR to 2,27,642 $/hr with EIR, indicating a major impact of reliability considerations. The real power loss values also increase when EIR is considered, though the magnitude of increase varies across cases and algorithms. For instance, in Case_1, the real power loss remains relatively low at 0.66037 kW (ILOA) without EIR, but with EIR, it is slightly reduced to 0.6141 kW. This suggests that in some cases, EIR can actually help optimize power loss while still increasing costs. However, in higher load cases like Case_7, the power loss increases from 71.07 kW to 69.82 kW with EIR, showing that reliability considerations do not always lead to higher losses, but often create a trade-off between cost and loss performance.

Across both single and multi-objective optimization frameworks, including EIR consistently raises operational costs, reflecting the additional constraints imposed by reliability. While most cases show an increase in power loss with EIR, some cases (such as Case_1) exhibit reduced power loss, highlighting non-linear interactions between DG scheduling, reliability, and power flow optimization. Unlike single-objective optimization, where either cost or loss is minimized independently, the multi-objective approach balances the two, resulting in compromise solutions that reflect real-world trade-offs. ILOA consistently achieves lower operating costs compared to LOA, JAYA, and GA, making it an optimal choice for economic DG scheduling. In many scenarios, ILOA maintains lower real power losses**,** ensuring higher energy efficiency. Unlike traditional optimization methods that prioritize global solutions, ILOA achieves a more balanced approach between cost efficiency and power loss reduction.

Conclusion and directions for future research

This paper proposed the Improved Lyrebird Optimization Algorithm (ILOA) as a robust and efficient solution for the optimal sectionalizing and scheduling of multi-microgrid systems.

- The algorithm effectively minimized generation costs and active power losses while addressing reliability constraints, such as the Energy Index of Reliability (EIR), and ensured stable system performance with renewable energy integration.
- By integrating advanced mechanisms like Levy Flight for enhanced local search and a chaotic sine map for improved global exploration, ILOA achieved faster convergence and superior optimization results compared

to conventional algorithms like the Genetic Algorithm (GA), Jaya Algorithm (JAYA), and the original Lyrebird Optimization Algorithm (LOA).
- Simulation results on a modified 33-bus distribution system, segmented into three independent microgrids, demonstrated the practical applicability of ILOA in both single-objective and multi-objective optimization scenarios.
- In single-objective cases, the algorithm achieved notable improvements in generation cost and active power loss reduction. In multi-objective optimization, it balanced these objectives more effectively than competing methods, further validating its robustness and effectiveness.
- For the IEEE-33 bus system under multi-objective optimization without considering EIR, the proposed ILOA algorithm significantly enhances system performance by reducing generation cost by approximately 0.1062%, 1.0822%, and 1.5318% compared to LOA, JAYA, and GA, respectively. Additionally, ILOA lowers active power loss by around 0.5968%, 1.942%, and 1.3891% relative to LOA, JAYA, and GA, respectively, under the operational scenario of Case-7. These results highlight the effectiveness of ILOA in optimizing both economic and technical parameters in power system operation.
- For the IEEE-33 bus system with considering EIR, the proposed ILOA algorithm achieves generation cost savings of approximately 0.0057% and 0.0214% compared to LOA and JAYA, respectively. Additionally, ILOA demonstrates a notable reduction in active power loss by 4.07% and 8.47% compared to LOA and JAYA, respectively, under the operational scenario of Case-7. These findings further validate the effectiveness of ILOA in optimizing economic and technical performance in power systems.
- While the results highlighted the significant potential of ILOA, certain limitations remained. The scalability of the algorithm to larger, more complex systems and its adaptability to dynamic and uncertain grid conditions warranted further exploration.

Additionally, the incorporation of constraint-handling mechanisms, such as reliability indices and advanced forecasting techniques for renewable energy sources, could have enhanced its robustness.Future work could focus on leveraging real-time grid data and integrating machine learning techniques to improve decision-making under uncertainty. Exploring hybrid frameworks combining ILOA with methods like game theory or reinforcement learning could extend its application to more complex objectives, including energy storage management, demand response, and fault detection in multi-microgrid systems. The ILOA showcased its capability as an efficient and reliable method for optimizing distributed generation scheduling and sectionalizing multi-microgrid systems, highlighting its promise as a key enabler for future advancements in smart grid applications.

Data availability

The datasets used and/or analysed during the current study available from the corresponding author on reasonable request.

Received: 24 January 2025; Accepted: 12 May 2025
Published online: 19 May 2025

References

1. Rajagopalan, A. et al. Multi-objective optimal scheduling of a microgrid using oppositional gradient-based grey wolf optimizer. *Energies* **15**(23), 9024 (2022).
2. Nagarajan, K. et al. (2024). Optimal scheduling of a microgrid incorporating renewables and demand response using a new heuristic optimization technique. *Biomass Solar Powered Sustain. Digit. Cities*, 255–284.
3. Nagarajan, K., Rajagopalan, A., Angalaeswari, S., Natrayan, L. & Mammo, W. D. Combined economic emission dispatch of microgrid with the incorporation of renewable energy sources using improved mayfly optimization algorithm. *Comput. Intell. Neurosci.* **2022**(1), 6461690 (2022).
4. Mei, Y., Li, B., Wang, H., Wang, X. & Negnevitsky, M. Multi-objective optimal scheduling of microgrid with electric vehicles. *Energy Rep.* **8**, 4512–4524 (2022).
5. Basu, M. Dynamic optimal power flow for grid-connected multi-microgrid system considering outage of energy sources. *Electric Power Components Syst.* 1–21 (2023).
6. Bidgoli, M. A. & Ahmadian, A. Multi-stage optimal scheduling of multi-microgrids using deep-learning artificial neural network and cooperative game approach. *Energy* **239**, 122036 (2022).
7. Baghbanzadeh, D., Salehi, J., Gazijahani, F. S., Shafie-khah, M. & Catalão, J. P. Resilience improvement of multi-microgrid distribution networks using distributed generation. *Sustain. Energy, Grids Netw.* **27**, 100503 (2021).
8. Bayat, P., Afrakhte, H. & Bayat, P. Reliability-oriented operation of distribution networks with multi-microgrids considering peer-to-peer energy sharing. *Sustain. Energy, Grids Netw.* **28**, 100530 (2021).
9. Afrakhte, H. & Bayat, P. A contingency based energy management strategy for multi-microgrids considering battery energy storage systems and electric vehicles. *J. Energy Storage* **27**, 101087 (2020).
10. Mehraban, S. A. & Eslami, R. Multi-microgrids energy management in power transmission mode considering different uncertainties. *Electric Power Syst. Res.* **216**, 109071 (2023).
11. Roustaee, M. & Kazemi, A. Multi-objective stochastic operation of multi-microgrids constrained to system reliability and clean energy based on energy management system. *Electric Power Syst. Res.* **194**, 106970 (2021).
12. Yang, D., Zhang, C., Jiang, C., Liu, X. & Shen, Y. Interval method based optimal scheduling of regional multi-microgrids with uncertainties of renewable energy. *IEEE Access* **9**, 53292–53305 (2021).
13. Villanueva-Rosario, J. A., Santos-García, F., Aybar-Mejía, M. E., Mendoza-Araya, P. & Molina-García, A. Coordinated ancillary services, market participation and communication of multi-microgrids: A review. *Appl. Energy* **308**, 118332 (2022).
14. Saha, D., Bazmohammadi, N., Vasquez, J. C. & Guerrero, J. M. Multiple microgrids: A review of architectures and operation and control strategies. *Energies* **16**(2), 600 (2023).
15. Yang, M., Cui, Y. & Wang, J. Multi-Objective optimal scheduling of island microgrids considering the uncertainty of renewable energy output. *Int. J. Electr. Power Energy Syst.* **144**, 108619 (2023).
16. Mishra, D. K., Ghadi, M. J., Li, L., Zhang, J. & Hossain, M. J. Active distribution system resilience quantification and enhancement through multi-microgrid and mobile energy storage. *Appl. Energy* **311**, 118665 (2022).

17. Bo, Y., Xia, Y., Wei, W., Li, Z. & Zhou, Y. Peer-to-peer electricity-hydrogen energy trading for multi-microgrids based on purification sharing mechanism. *Int. J. Electr. Power Energy Syst.* **150**, 109113 (2023).
18. Masrur, H. et al. An optimized and outage-resilient energy management framework for multicarrier energy microgrids integrating demand response. *IEEE Trans. Ind. Appl.* **58**(3), 4171–4180 (2022).
19. Yammani, C. & Prabhat, P. Reliability improvement of future microgrid with mixed load models by optimal dispatch of DGs. *Int. Trans. Electr. Energy Syst.* **29**(4), e2816 (2019).
20. Shezan, S. A. et al. Evaluation of different optimization techniques and control strategies of hybrid microgrid: A review. *Energies* **16**(4), 1792 (2023).
21. Ma, G., Li, J. & Zhang, X. P. A review on optimal energy management of multi microgrid system considering uncertainties. *IEEE Access* **10**, 77081–77098 (2022).
22. Mukhopadhyay, B. & Das, D. Optimal multi-objective long-term sizing of distributed energy resources and hourly power scheduling in a grid-tied microgrid. *Sustain. Energy, Grids Netw.* **30**, 100632 (2022).
23. Ashtari, B. et al. A two-stage energy management framework for optimal scheduling of multi-microgrids with generation and demand forecasting. *Neural Comput. Appl.* **34**, 12159–12173. https://doi.org/10.1007/s00521-022-07103-w (2022).
24. Paul, K. et al. Optimizing sustainable energy management in grid connected microgrids using quantum particle swarm optimization for cost and emission reduction. *Sci. Rep.* **15**(1), 5843 (2025).
25. Phommixay, S., Doumbia, M. L. & Lupien St-Pierre, D. Review on the cost optimization of microgrids via particle swarm optimization. *Int. J. Energy Environ. Eng.* **11**(1), 73–89 (2020).
26. Singh, A. R. et al. Advanced microgrid optimization using price-elastic demand response and greedy rat swarm optimization for economic and environmental efficiency. *Sci. Rep.* **15**(1), 2261 (2025).
27. Nguyen, T. A. & Crow, M. L. Stochastic optimization of renewable-based microgrid operation incorporating battery operating cost. *IEEE Trans. Power Syst.* **31**(3), 2289–2296 (2015).
28. Singh, A. R. et al. A hybrid demand-side policy for balanced economic emission in microgrid systems. *iScience.* **28**, 112121 (2025).
29. Selvaraj, G. et al. Optimal power scheduling in real-time distribution systems using crow search algorithm for enhanced microgrid performance. *Sci. Rep.* **14**(1), 30982 (2024).
30. Garcia-Torres, F. et al. Stochastic optimization of microgrids with hybrid energy storage systems for grid flexibility services considering energy forecast uncertainties. *IEEE Trans. Power Syst.* **36**(6), 5537–5547 (2021).
31. Nadimuthu, L. P. R., Victor, K., Bajaj, M. & Tuka, M. B. Feasibility of renewable energy microgrids with vehicle-to-grid technology for smart villages: A case study from India. *Res. Eng.* **24**, 103474 (2024).
32. Singh, R. et al. Machine learning-based energy management and power forecasting in grid-connected microgrids with multiple distributed energy sources. *Sci. Rep.* **14**(1), 19207 (2024).
33. Ott, M., AlMuhaini, M. & Khalid, M. A MILP-based restoration technique for multi-microgrid distribution systems. *IEEE Access* **7**, 136801–136811 (2019).
34. Karthik, N. et al. Chaotic self-adaptive sine cosine multi-objective optimization algorithm to solve microgrid optimal energy scheduling problems. *Sci. Rep.* **14**(1), 18997 (2024).
35. Abdalla, A. N. et al. Optimized economic operation of microgrid: combined cooling and heating power and hybrid energy storage systems. *J. Energy Res. Technol.* **143**(7), 070906 (2021).
36. Artis, R., Assili, M. & Shivaie, M. A seismic-resilient multi-level framework for distribution network reinforcement planning considering renewable-based multi-microgrids. *Appl. Energy* **325**, 119824 (2022).
37. Rajagopalan, A. et al. Multi-objective energy management in a renewable and EV-integrated microgrid using an iterative map-based self-adaptive crystal structure algorithm. *Sci. Rep.* **14**(1), 15652 (2024).
38. Arefifar, S. A., Ordonez, M. & Mohamed, Y. A. R. I. Voltage and current controllability in multi-microgrid smart distribution systems. *IEEE Trans. Smart Grid* **9**(2), 817–826 (2016).
39. Malik, M. M., Kazmi, S. A. A., Asim, H. W., Ahmed, A. B. & Shin, D. R. An intelligent multi-stage optimization approach for community based micro-grid within multi-microgrid paradigm. *IEEE Access* **8**, 177228–177244 (2020).
40. He, Y. et al. Economic optimization scheduling of multi-microgrid based on improved genetic algorithm. *IET Gener. Transm. Distrib.* **17**(23), 5298–5307 (2023).
41. Srinivasarathnam, C., Yammani, C. & Maheswarapu, S. Multi-objective jaya algorithm for optimal scheduling of DGs in distribution system sectionalized into multi-microgrids. *Smart Sci.* https://doi.org/10.1080/23080477.2018.1540381 (2018).
42. Aghdam, F. H., Kalantari, N. T. & Mohammadi-Ivatloo, B. A stochastic optimal scheduling of multi-microgrid systems considering emissions: A chance constrained model. *J. Clean. Prod.* **275**, 122965 (2020).
43. Sarshar, J., Moosapour, S. S. & Joorabian, M. Multi-objective energy management of a micro-grid considering uncertainty in wind power forecasting. *Energy* **139**, 680–693 (2017).
44. Xu, J., Li, K. & Abusara, M. Preference based multi-objective reinforcement learning for multi-microgrid system optimization problem in smart grid. *Memetic Comput.* **14**(2), 225–235 (2022).
45. Indragandhi, V. et al. Multi-objective optimization and energy management in renewable based AC/DC microgrid. *Comput. Electr. Eng.* **70**, 179–198 (2018).
46. Mu, C. et al. Multi-objective interval optimization dispatch of microgrid via deep reinforcement learning. *IEEE Trans. Smart Grid* **15**, 2957–2970 (2024).
47. Li, Y., Wang, R. & Yang, Z. Optimal scheduling of isolated microgrids using automated reinforcement learning-based multi-period forecasting. *IEEE Trans. Sustain. Energy* **13**(1), 159–169 (2022).
48. Hussain, A. & Kim, H. M. Goal-programming-based multi-objective optimization in off-grid microgrids. *Sustainability* **12**(19), 8119 (2020).
49. Carpinelli, G., Mottola, F., Proto, D. & Russo, A. A multi-objective approach for microgrid scheduling. *IEEE Trans. Smart Grid* **8**(5), 2109–2118 (2016).
50. Karimi, H. & Jadid, S. Two-stage economic, reliability, and environmental scheduling of multi-microgrid systems and fair cost allocation. *Sustain. Energy, Grids Netw.* **28**, 100546 (2021).
51. Chakraborty, A. & Ray, S. Multi-objective operational cost management with minimum net emission of a smart microgrid. *Electric Power Compon Syst.* **52**(10), 1870–1891 (2024).
52. Ghiasi, M. et al. Optimal multi-operation energy management in smart microgrids in the presence of RESs based on multi-objective improved de algorithm: Cost-emission based optimization. *Appl. Sci.* **11**(8), 3661 (2021).
53. BabanezhaadShirdar, H. & Ghafouri, A. Optimization of multi-microgrid system operation cost with different energy management tools in the presence of energy storage system. *Electric Power Compon. Syst.* **50**(16–17), 951–971 (2022).
54. Guan, Z. et al. Multi-Objective optimal scheduling of microgrids based on improved particle swarm algorithm. *Energies* **17**(7), 1760 (2024).
55. Song, X., Qu, Z., Wang, Y. & Chong, Z. Optimization of multi-energy cloud energy storage for multi-microgrid system with hydrogen refueling station. *Renew. Energy* **241**, 122382 (2025).
56. Seyednouri, S. R. et al. Day-ahead scheduling of multi-energy microgrids based on a stochastic multi-objective optimization model. *Energies* **16**(4), 1802 (2023).
57. Pan, Y., Ju, L., Yang, S., Guo, X. & Tan, Z. A multi-objective robust optimal dispatch and cost allocation model for microgrids-shared hybrid energy storage system considering flexible ramping capacity. *Appl. Energy* **369**, 123565 (2024).

58. Li, G., Lin, X., Kong, L., Xia, W. & Yan, S. Enhanced bi-level optimal scheduling strategy for distribution network with multi-microgrids considering source-load uncertainties. *Front. Energy Res.* **12**, 1413935 (2024).
59. Hou, J., Yang, W., Qian, H., Li, Z. & Cai, J. Distributionally robust optimal scheduling of multi-microgrid considering asymmetric bargaining. *Electric Power Syst. Res.* **229**, 110211 (2024).
60. Zhu, X. et al. Multi-objective sizing optimization method of microgrid considering cost and carbon emissions. *IEEE Trans. Ind. Appl.* **60**, 5565–5576 (2024).
61. Wu, N., Xu, J., Linghu, J. & Huang, J. Real-time optimal control and dispatching strategy of multi-microgrid energy based on storage collaborative. *Int. J. Electr. Power Energy Syst.* **160**, 110063 (2024).
62. Wu, X., Li, S., He, P., Zhao, C., & Liu, M. Economic dispatch of multi-microgrids considering flexible load based on distributed consensus algorithm. *Electr. Eng.* 1–12 (2024).
63. Yan, D., Wang, H., Gao, Y., Tian, S. & Zhang, H. Based on improved crayfish optimization algorithm cooperative optimal scheduling of multi-microgrid system. *Sci. Rep.* **14**(1), 24871 (2024).
64. Huang, J., Guo, H. & Luo, H. Economic optimization scheduling strategy for offshore fishing raft microgrid clusters. *IEEE Access.* **12**, 76986–76994 (2024).
65. Gao, X. & Zhang, X. Robust collaborative scheduling strategy for multi-microgrids of renewable energy based on a non-cooperative game and profit allocation mechanism. *Energies* **17**(2), 519 (2024).
66. Kalantari, A. & Lesani, H. Operation scheduling of distribution network with photovoltaic/wind/battery multi-microgrids and reconfiguration considering reliability and self-healing. *Int. J. Energy Res.* **2024**(1), 5724653 (2024).
67. Chakraborty, A. & Ray, S. Economic and environmental factors based multi-objective approach for optimizing energy management in a microgrid. *Renew. Energy* **222**, 119920 (2024).
68. Sun, Y. et al. Multi-objective optimal scheduling for microgrids—improved goose algorithm. *Energies* **17**(24), 6376 (2024).
69. Jasim, A. M., Jasim, B. H., Kraiem, H. & Flah, A. A multi-objective demand/generation scheduling model-based microgrid energy management system. *Sustainability* **14**(16), 10158 (2022).
70. Karthik, N., Parvathy, A. K., Arul, R., spsampsps Padmanathan, K. Levy interior search algorithm-based multi-objective optimal reactive power dispatch for voltage stability enhancement. In *Advances in Smart Grid Technology: Select Proceedings of PECCON 2019—Volume II* 221–244 (Springer Singapore, 2021).
71. Srinivasarathnam, C., Yammani, C., & Maheswarapu, S. Multi-objective optimal scheduling of microsources in distribution system based on sectionalization into microgrid. In *2018 International Conference on Sustainable Energy, Electronics, and Computing Systems (SEEMS)* 1–5 (IEEE, 2018).
72. Rathnam, C. S., Annamraju, A., Gurappa, B., Yammani, C., & Salkuti, S. R. Optimal Scheduling of Micro-sources in Multi-microgrid System. In *Power Quality in Microgrids: Issues, Challenges and Mitigation Techniques* 243–27) (Springer Nature Singapore, Singapore, 2023).
73. Srinivasarathnam, C., Yammani, C., & Maheswarapu, S. Optimal scheduling of micro-sources in multi-microgrids for reliability improvement. In *2019 National Power Electronics Conference (NPEC)* 1–6. (IEEE, 2019).
74. Mohseni-Bonab, S. M., Rabiee, A., Jalilzadeh, S., Mohammadi-Ivatloo, B. & Nojavan, S. Probabilistic multi objective optimal reactive power dispatch considering load uncertainties using Monte Carlo simulations. *J. Oper. Autom. Power Engg.* **3**(1), 83–93 (2015).
75. Deb K. Multi-objective optimization using evolutionary algorithms (John Wiley & Sons, 2001).
76. Rabiee, A., Soroudi, A., Mohammadi-Ivatloo, B. & Parniani, M. Corrective voltage control scheme considering demand response and stochastic wind power. *IEEE Trans. Power Syst.* **29**(6), 2965–2973 (2014).
77. Venkatesh, P., Gnanadass, R. & Padhy, N. P. Comparison and application of evolutionary programming techniques to combined economic emission dispatch with line flow constraints. *IEEE Trans. Power Syst.* **18**(2), 688–697 (2003).
78. Nagarajan, K., Parvathy, A. K. & Rajagopalan, A. Multi-objective optimal reactive power dispatch using levy interior search algorithm. *Int. J. Electr. Eng. Inf.* **12**(3), 547–570 (2020).
79. Rabiee, A., Soroudi, A., Mohammadi-Ivatloo, B. & Parniani, M. Corrective voltage control scheme considering demand response and stochastic wind power. *IEEE Trans Power Syst.* **29**, 2965–2973 (2014).
80. Mohseni-Bonab, S. M. et al. A two-point estimate method for uncertainty modeling in multi-objective optimal reactive power dispatch problem. *Electr. Power Energy Syst.* **75**, 194–204 (2016).
81. Dehghani, M. et al. Lyrebird optimization algorithm: a new bio-inspired metaheuristic algorithm for solving optimization problems. *Biomimetics* **8**(6), 507 (2023).
82. Nagarajan, K. et al. Optimizing dynamic economic dispatch through an enhanced Cheetah-inspired algorithm for integrated renewable energy and demand-side management. *Sci. Rep.* **14**(1), 3091 (2024).
83. Nagarajan, K., Rajagopalan, A., Selvaraj, P., Ravi, H. K., & Kareem, I. A. Demand Response-Integrated Economic Emission Dispatch Using Improved Remora Optimization Algorithm. In *AI Approaches to Smart and Sustainable Power Systems* 120–140. (IGI Global, 2024)
84. Hakli, H. & Uguz, H. A novel particle swarm optimization algorithm with Levy flight. *Appl. Soft Comput.* **23**(1), 333–345 (2014).
85. Chechkin, A. V., Metzler, R., Klafter, J. & Gonchar, V. Y. Introduction To The Theory of Levy Flights. In *Anomalous Transport: Foundations and Applications* (eds Klages, R. et al.) 129–162 (John Wiley & Sons, 2008).
86. Karthik, N., A. K. et al. A New Heuristic Algorithm for Economic Load Dispatch Incorporating Wind Power. In *Artificial Intelligence and Evolutionary Computations in Engineering Systems: Computational Algorithm for AI Technology, Proceedings of ICAIECES 2020*,47–65. (Springer Singapore, 2022).
87. Karthik, N., Rajagopalan, A., Prakash, V. R., Montoya, O. D., Sowmmiya, U., & Kanimozhi, R. Environmental Economic Load Dispatch Considering Demand Response Using a New Heuristic Optimization Algorithm. In *AI Techniques for Renewable Source Integration and Battery Charging Methods in Electric Vehicle Applications*, 220–242 (2023).
88. Arora, K. et al. Optimization methodologies and testing on standard benchmark functions of load frequency control for interconnected multi area power system in smart grids. *Mathematics* **8**(6), 980 (2020).
89. Li, F., Shen, W., Cai, X., Gao, L. & Wang, G. G. A fast surrogate-assisted particle swarm optimization algorithm for computationally expensive problems. *Appl. Soft Comput.* **92**, 106303 (2020).
90. Naderi, E., Mirzaei, L., Trimble, J. P. & Cantrell, D. A. Multi-objective optimal power flow incorporating flexible alternating current transmission systems: Application of a wavelet-oriented evolutionary algorithm. *Electric Power Compon. Syst.* **52**(5), 766–795. https://doi.org/10.1080/15325008.2023.2234378 (2024).
91. Li, L., Zhou, Y. & Xie, J. A free search krill herd algorithm for functions optimization. *Math. Probl. Eng.* **2014**(1), 936374 (2014).
92. Naderi, E., Mirzaei, L., Pourakbari-Kasmaei, M., Cerna, F. V. & Lehtonen, M. Optimization of active power dispatch considering unified power flow controller: Application of evolutionary algorithms in a fuzzy framework. *Evol. Intel.* **17**(3), 1357–1387 (2024).

Acknowledgements

This research is funded by European Union under the REFRESH—Research Excellence For Region Sustainability and High-Tech Industries Project via the Operational Programme Just Transition under Grant CZ.10.03.01/00/22_003/0000048; in part by the National Centre for Energy II and ExPEDite Project a Research and Innovation Action to Support the Implementation of the Climate Neutral and Smart Cities Mission Project

TN02000025; and in part by ExPEDite through European Union's Horizon Mission Programme under Grant 101139527. The authors would like to express their sincere gratitude to Stanislav Misak for his exceptional supervision, project administration, and overall guidance throughout the course of this project. His expertise and support were instrumental to its success. The authors also wish to thank the Hindustan Institute of Technology & Science, Chennai, India, Vellore Institute of Technology, Chennai, India, and Perdana University, Kuala Lumpur, Malaysia for their all support and encouragement to carry out this work.

Author contributions

K.N., A.R.: Conceptualization, Methodology, Software, Visualization, Investigation, Writing—Original draft preparation. V.R.: Data curation, Validation, Supervision, Resources, Writing—Review & Editing. M.B., V.B., L.P.: Project administration, Supervision, Resources, Writing—Review & Editing.

Declarations

Competing interests

The authors declare no competing interests.

Additional information

Correspondence and requests for materials should be addressed to A.R. or M.B.

Reprints and permissions information is available at www.nature.com/reprints.

Publisher's note Springer Nature remains neutral with regard to jurisdictional claims in published maps and institutional affiliations.